# Making sense of astrocytic calcium signals — from acquisition to interpretation

*Alexey Semyanov*[1,2,8]✉, *Christian Henneberger*[3,4,5,8]✉ *and Amit Agarwal*[6,7,8]✉

Abstract | Astrocytes functionally interact with neurons and with other brain cells. Although not electrically excitable, astrocytes display a complex repertoire of intracellular $Ca^{2+}$ signalling that evolves in space and time within single astrocytes and across astrocytic networks. Decoding the physiological meaning of these dynamic changes in astrocytic $Ca^{2+}$ activity has remained a major challenge. This Review describes experimental preparations and methods for recording and studying $Ca^{2+}$ activity in astrocytes, focusing on the analysis of $Ca^{2+}$ signalling events in single astrocytes and in astrocytic networks. The limitations of existing experimental approaches and ongoing technical and conceptual challenges in the interpretation of astrocytic $Ca^{2+}$ events and their spatio-temporal patterns are also discussed.

Intracellular $Ca^{2+}$ signals in astrocytes are vital for the optimal functioning of the CNS[1,2] and represent the astrocytic counterpart of neuronal membrane potential changes such as action potentials. However, the properties, underlying mechanisms, physiological and pathophysiological significance and putative information content of astrocytic $Ca^{2+}$ signals are far less thoroughly understood than neuronal excitability. The accelerating pace of development of optical imaging techniques and the emergence of several unexpected observations have put $Ca^{2+}$ signalling at the centre of debates on the molecular and cellular aspects of astrocyte physiology. Hence, decoding astrocytic $Ca^{2+}$ signalling is an immediate and important challenge in modern neurobiology.

Neuronal physiology was primarily elucidated by use of electrophysiological methods; refinement of these approaches led to important advances such as the invention of the patch clamp technique. These methods have also greatly contributed to studying the role of astrocytes in regulating synaptic transmission and neuronal excitability[3]. The development of advanced optical imaging techniques (such as two-photon excitation fluorescence imaging) and sensitive genetically encoded $Ca^{2+}$ indicators (GECIs), which change their fluorescence properties on binding to $Ca^{2+}$ ions, enabled the visualization of intracellular $Ca^{2+}$ concentrations in electrically non-excitable astrocytes. As a result, astrocytes were discovered to possess complex ionic signalling mechanisms, including some involving $Ca^{2+}$. The $Ca^{2+}$ signals were found to have highly regulated spatial and temporal dynamics that were not amenable to investigation using electrode-based methods.

This Review focuses on how these technological advances have reshaped our understanding of astrocytic $Ca^{2+}$ signalling. Specifically, we describe the key properties of astrocytic $Ca^{2+}$ signals and the mechanisms that generate and shape them in space and time, and discuss how these signals interact and spread in individual astrocytes and astrocytic networks. Finally, we explore the computational properties of $Ca^{2+}$ signalling in astrocytic networks and consider how these compare with established concepts in neuronal signalling. To what extent these properties are dependent on neuronal circuit activity and sensory input is also addressed.

## Experimental preparations

Experimental preparations using a variety of $Ca^{2+}$ indicators, each with their own advantages and limitations, have been used to explore $Ca^{2+}$ signalling dynamics. Astrocytic $Ca^{2+}$ activity has been successfully studied across many species from *Drosophila*[4], zebrafish[5], rodents and ferrets[6] to humans[7]. However, most of the experiments described in this Review were performed in rodents as the most commonly used model organism in neurobiology.

***Cell cultures.*** Pioneering work on astrocyte physiology began on cultured cells at the beginning of the 1990s, when astrocytes were first observed to generate spontaneous $Ca^{2+}$ transients[8]. As astrocytes in a pure monolayer culture do not develop the complex morphology characteristic of their in vivo counterparts, most $Ca^{2+}$ activity in cultured astrocytes either occupies the entire cell or occurs close to the plasma membrane[9]. These $Ca^{2+}$ signals

✉*e-mail: semyanov@ibch.ru; christian.henneberger@uni-bonn.de; amit.agarwal@uni-heidelberg.de*

https://doi.org/10.1038/s41583-020-0361-8

are qualitatively different from those observed in intact preparations (FIG. 1). This difference could be caused by many factors, including alterations in the geometry of the cytosol or in the spatial distribution of crucial $Ca^{2+}$ signalling components (such as $Ca^{2+}$ stores, pumps and buffers), or atypical expression of receptors and channels compared with astrocytes in vivo[10,11]. Nonetheless, cell culture systems remain a powerful tool for dissecting fundamental cellular pathways. Improved culture methods are pushing astrocytes towards in vivo-like characteristics[12].

***Brain slices.*** Acute brain slices are another widely used preparation that offers the advantage that cells and their connections originally developed in their natural in vivo environment. Astrocytes in brain slices retain highly ramified processes (branchlets) and thin protrusions that contact synapses (leaflets) and blood vessels (end-feet), the morphological characteristics of in vivo tissue[13–16], and exhibit focally restricted and complex $Ca^{2+}$ activity patterns[17–19] (FIG. 1). As local neuronal circuitry and the spatial arrangement of the various cell types in the neuropile are largely preserved in brain slice preparations, they have been instrumental in uncovering the basic mechanisms that drive astrocytic $Ca^{2+}$ signalling and in revealing how these depend on neuronal activity[18,20–23]. However, the disruption of long-range connectivity during tissue preparation limits the usefulness of brain slices beyond the study of astrocytes within their local cell assemblies. Moreover, tissue damage during slice preparation can potentially trigger reactive astrogliosis, which might change astrocyte physiology[24]. Nonetheless, acute brain slices remain ideally suited for studying the interactions between neurons and astrocytes by electrophysiological, optical and combined methods at high spatial and temporal resolution, and for local and targeted manipulations.

***Intravital preparations.*** The advent of two-photon excitation fluorescence microscopy enabled the recording and correlation of in vivo astrocytic $Ca^{2+}$ activity with neuronal activation[25,26] (FIG. 1). Most of the early in vivo imaging experiments were performed in anaesthetized animals. However, researchers soon realized that general anaesthetics suppress astrocytic $Ca^{2+}$ signalling[27]. With advances in imaging methods, in vivo approaches evolved towards studies in awake and behaving animals[28–32]. Several configurations for imaging of head-fixed, awake mice have been developed, such as an air-suspended Styrofoam ball, a mobile home cage and a treadmill or running disc combined with virtual reality[28,33–35]. However, craniotomy and implantation of the glass window can still trigger reactive astrogliosis and potentially change the physiology of astrocytes. This issue can be overcome by use of thinned-skull preparations, albeit at the expense of reductions in spatial resolution and the imaging time frame[36]. Thus, despite the limited amenability of in vivo preparations to pharmacological and electrophysiological experimentation, they remain the tool of choice to study astrocytic $Ca^{2+}$ signals in the intact brain and during defined behavioural paradigms.

***Induced astrocytes.*** Astrocytes in primates, including humans, are divided into various anatomical classes[37,38] and express several genes that are not expressed in the astrocytes of other mammals (reviewed elsewhere[39]). In addition to the anatomical astrocyte classes present in both humans and mice (namely Bergmann glia, fibrous astrocytes, protoplasmic astrocytes and velate astrocytes), the primate cortex contains two unique astrocyte classes: varicose projection astrocytes and interlaminar astrocytes. Hence, the outcomes of studies of rodent astrocytes, especially those in rodent models of disease, might not be generalizable to human astrocytes. Access to human brain tissue is limited to surgical biopsy samples obtained during resection of tumours or epileptic foci. Whether the data obtained from such patient-derived tissue samples (which have usually been exposed to various medications) capture the physiological properties of astrocytes in the healthy human brain remains an open question[7,37,39]. A promising approach to study the basic physiology of human astrocytes is direct genetic reprogramming of either human embryonic stem cells or induced pluripotent stem cells into astrocytes[40]. However, the functionality of such astrocytes needs to be extensively validated[41].

Moving towards ever more advanced experimental paradigms in intact preparations might intuitively be expected to be the key to understanding fundamental principles of astrocytic $Ca^{2+}$ signalling. However, these advances come at the expense of the very restricted toolsets for manipulating $Ca^{2+}$ signals in these preparations, compared with those available for simpler experimental set-ups. Hence, to fully decode $Ca^{2+}$ signalling mechanisms in astrocytes it is essential to integrate the results obtained from several different preparations.

## Visualizing astrocytic $Ca^{2+}$ signals

Overall, the experimental techniques for monitoring astrocytic $Ca^{2+}$ dynamics by fluorescence microscopy do not differ from those in other areas of neuroscience and biology. Approaches for introducing $Ca^{2+}$-sensitive fluorescent dyes into cells are summarized in TABLE 1. In the following sections, we highlight a few key aspects that can substantially affect calcium imaging results and their interpretation.

***The dimensionality of $Ca^{2+}$ events.*** Changes in the cytosolic $Ca^{2+}$ concentration in astrocytes occur in three spatial dimensions and over time. Thus, each event can have a characteristic spread, speed and temporal

**Author addresses**

[1]Shemyakin-Ovchinnikov Institute of Bioorganic Chemistry, Russian Academy of Sciences, Moscow, Russia.
[2]Sechenov First Moscow State Medical University, Moscow, Russia.
[3]Institute of Cellular Neurosciences, Medical Faculty, University of Bonn, Bonn, Germany.
[4]Institute of Neurology, University College London, London, UK.
[5]German Center for Neurodegenerative Diseases (DZNE), Bonn, Germany.
[6]The Chica and Heinz Schaller Research Group, Institute for Anatomy and Cell Biology, Heidelberg University, Heidelberg, Germany.
[7]Interdisciplinary Center for Neurosciences, Heidelberg University, Heidelberg, Germany.
[8]These authors contributed equally: Alexey Semyanov, Christian Henneberger, Amit Agarwal.

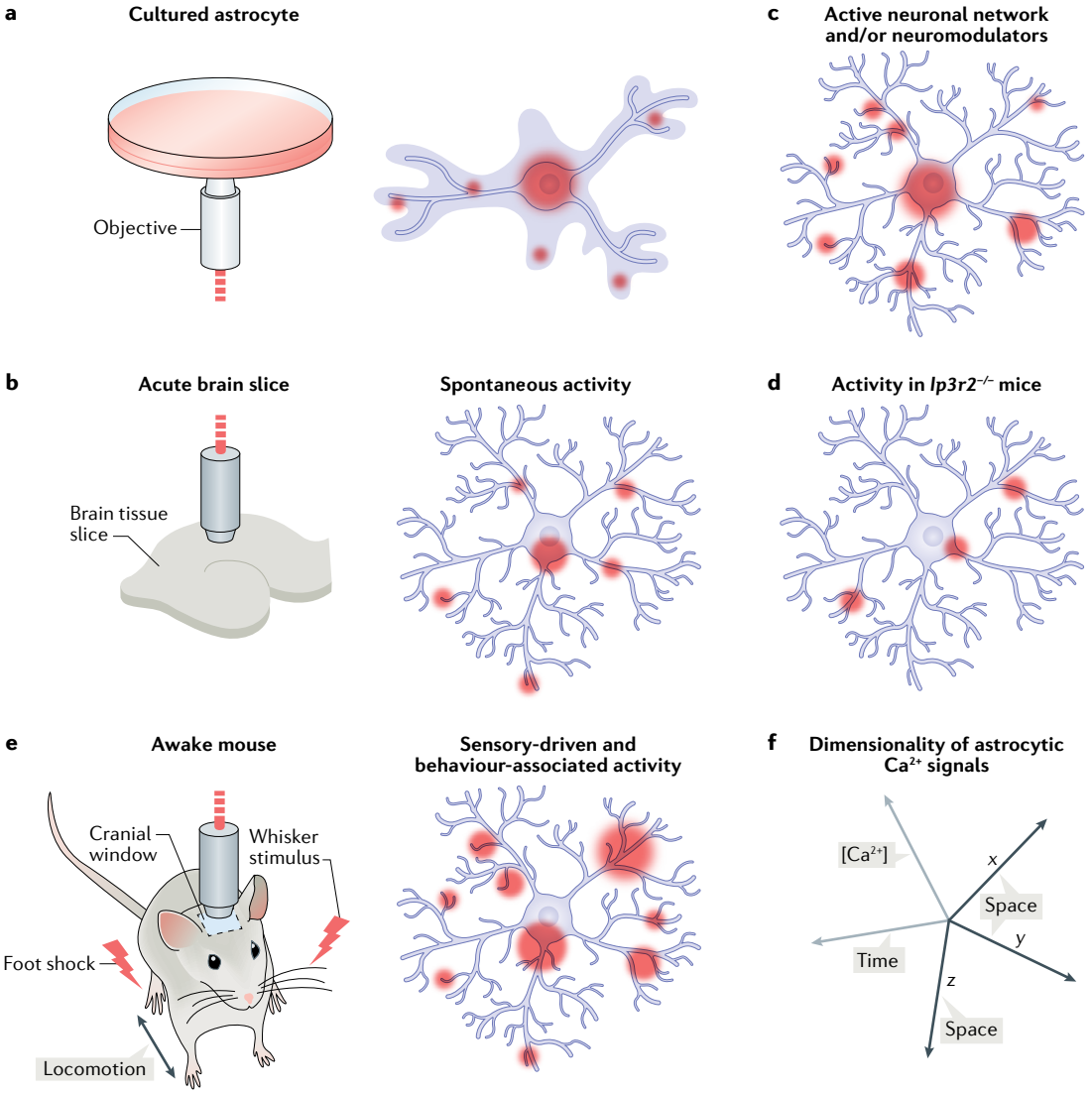


Fig. 1 | **Visualization of astrocytic $Ca^{2+}$ signals. a** | Cultured astrocytes typically develop a very different morphology to astrocytes either in vivo or in acute brain slices, characterized by few, if any, main processes (which are homologous to astrocytic branches in vivo) and the absence of leaflets. Instead, cultured astrocytes form a thin organelle-free protoplasmic cloud around their processes. A large number of small $Ca^{2+}$ events are triggered in this protoplasmic cloud, some of which are amplified and propagate through the processes and soma. **b** | Imaging of $Ca^{2+}$ events in brain slices (a hippocampal slice is depicted). Spontaneous $Ca^{2+}$ transients in quiescent ex vivo astrocytes occur predominantly in distal astrocytic processes and occasionally in the soma. **c** | Neuronal activity increases the spread and duration of spontaneous $Ca^{2+}$ events and also triggers new $Ca^{2+}$ events in astrocytes. Some $Ca^{2+}$ events in processes become sufficiently amplified to propagate all the way to the soma. **d** | Genetic deletion of inositol 1,4,5-trisphosphate receptor type 2 ($InsP_3R2$) (*Ip3r2*$^{-/-}$) in astrocytes dampens $Ca^{2+}$ events. Although spontaneous $Ca^{2+}$ events are considerably reduced, new events can still be triggered by $Ca^{2+}$ entry through the plasma membrane and $Ca^{2+}$ efflux from mitochondria. The absence of $InsP_3R2$ prevents the amplification (spreading and prolongation) of $Ca^{2+}$ events and the generation of new events that rely on $Ca^{2+}$ release from the endoplasmic reticulum. **e** | Imaging of $Ca^{2+}$ events in awake mice reveals astrocytic responses to sensory stimulation and behaviour (such as locomotion, foot shock and whisker stimulation). **f** | Each $Ca^{2+}$ signal can be characterized by several parameters: the magnitude of the elevation in $Ca^{2+}$ concentrations (amplitude), its spatial spread in three dimensions and its duration and temporal pattern. Within a given pattern of $Ca^{2+}$ activity, the event coordinates can also be defined within the astrocytic domain or within the local astrocytic network in both space and time.

profile (FIG. 1). However, astrocytic $Ca^{2+}$ events are mostly detected by monitoring the intensity of $Ca^{2+}$ indicator fluorescence in a single focal plane. Three-dimensional (3D) scanning enables information about $Ca^{2+}$ signal manifestations in a third dimension (the *z* axis) to be obtained[42]. However, stepwise frame-by-frame scanning along the z axis necessarily reduces the imaging speed of 3D scanning, meaning that rapid $Ca^{2+}$ events might go undetected. Decreasing the voxel dwell time can compensate for this inherent limitation of 3D imaging, albeit at the expense of collecting fewer photons per voxel, which inevitably means that small-amplitude (less bright) $Ca^{2+}$ events might go undetected. Furthermore, as each plane scanned along the *z* axis is imaged at a

Table 1 | **Fluorescent indicators for detecting astrocytic $Ca^{2+}$**

| Type | Examples | Advantages | Limitations | Refs |
|---|---|---|---|---|
| Membrane-permeable organic $Ca^{2+}$ indicators | AM ester dyes: Oregon Green, BAPTA AM and Fluo AM indicator families | Fluo-4 $Ca^{2+}$ binding and unbinding rates are superior to those of GECIs for fully resolving rapid $Ca^{2+}$ dynamics | Cell non-specific; co-staining with, for instance, sulforhodamine 101 (which can also stain oligodendrocytes and increase neuronal excitability); detects $Ca^{2+}$ signals only at the soma or large processes[a] | 8,18,115, 128–132 |
| Membrane-impermeable organic $Ca^{2+}$ indicators | Fluo and Oregon Green BAPTA indicator families, Fura-2 | Can be microinjected into individual cells; neighbouring astrocytes can also be imaged owing to dye diffusion through gap junctions; enables microinjection of $Ca^{2+}$ chelators and $Ca^{2+}$ signalling inhibitors; facilitates monitoring the activity and plasticity of nearby synapses | Dialysis of the cell and washout of proteins and possibly organelles could affect $Ca^{2+}$ activity in patch-clamped astrocytes | 18,44,125, 133,134 |
| Single-wavelength GECIs | GFP–calmodulin fusion proteins expressed using astrocyte-specific promoters (e.g. GFAP) in AAV vectors and Cre-dependent transgenic mice | Widely used to study astrocytic $Ca^{2+}$ transients; subcellular targeting sequences bound to GECIs enable recording of $Ca^{2+}$ dynamics from the membrane vicinity and within intracellular $Ca^{2+}$ stores such as mitochondria and ER | The $Ca^{2+}$-buffering effect of GECIs affects $Ca^{2+}$-dependent processes; mode and level of GECI expression can alter astrocyte behaviour; prolonged overexpression of modified GFP can induce a reactive phenotype; on their own, GECIs detect relative $Ca^{2+}$ changes rather than actual intracellular $Ca^{2+}$ concentrations | 9,31,45, 135–140 |
| Ratiometric GECIs | Yellow chamaeleon-Nano50[b] | More accurate measurement than with single-wavelength GECIs; single-wavelength GECI co-expressed with a reference fluorescent protein can be used for ratiometric imaging across cell subregions | The need for two distinct colour channels limits their use in multiplexed imaging (e.g. simultaneous imaging of neurons and astrocytes) | 32,135, 141,142 |

AAV, adeno-associated virus; AM, acetoxymethyl; BAPTA, 1,2-bis(*o*-aminophenoxy)ethane-*N*,*N*,*N*′,*N*′-tetraacetic acid; ER, endoplasmic reticulum; GECI, genetically encoded $Ca^{2+}$ indicator; GFAP, glial fibrillary acidic protein; GFP, green fluorescent protein. [a]Fluorescence originating from thin branchlets and leaflets cannot be distinguished from that of nearby neuronal structures. [b]Based on Förster resonance energy transfer.

different time, $Ca^{2+}$ signals that extend along the *z* axis might end before 3D scanning is complete. In addition, the tissue depth amenable to 3D imaging is limited by light scattering, with the consequence that the fluorescent signal collected from deep frames might not be directly comparable to that collected from frames near the surface during the same 3D scan. Finally, the highly non-linear relationship between indicator fluorescence and the actual $Ca^{2+}$ concentration in various cellular compartments is rarely considered (BOX 1). Thus, depending on the research question, single-plane or line-scan two-dimensonal imaging of astrocytic $Ca^{2+}$ signals (which can be done at faster rates than 3D imaging) might provide more reliable information than 3D scanning.

Quantitative imaging approaches can reveal otherwise undetectable basic properties of $Ca^{2+}$ signalling, including the resting $Ca^{2+}$ concentration in astrocytes[43,44]. These modalities were instrumental in showing that the resting $Ca^{2+}$ concentration controls the scale of local $Ca^{2+}$ signals, irrespective of whether they were triggered via various receptor pathways in vitro or by running of awake animals[32].

***Imaging resolution.*** Although astrocytic $Ca^{2+}$ signals are generally considered to be infrequent and to have slow kinetics, studies in ex vivo or in vivo rodent preparations using state-of-the-art GECIs and fast two-photon imaging have reported subsecond fluorescence transients, which still seem to be slower than those reported in neurons[19,45,46]. Further improvement in GECIs, their kinetics and imaging speeds could lead to the detection of even faster subsecond $Ca^{2+}$ transients. Alternatively, modelling of $Ca^{2+}$ transients and the kinetics of $Ca^{2+}$ binding to and unbinding from fluorescent indicators could lead to further insights into astrocytic $Ca^{2+}$ dynamics[47,48]. The subcellular distribution of $Ca^{2+}$ indicators (BOX 1) and the effective resolution of 3D imaging approaches also require consideration.

***Tissue heating and reactive oxygen species.*** Obtaining high-quality imaging data or performing optogenetic stimulation often requires prolonged exposure of cells to laser light. Astrocytes seem to be particularly sensitive to such extended exposures[49], which can increase the local temperature and activate heat-sensitive channels; ~30% of astrocytes in the mouse brain express transient receptor potential vanilloid 4 (TRPV4)[50,51]. Additionally, light exposure can induce excessive generation of intracellular reactive oxygen species (ROS), which can trigger $Ca^{2+}$ transients in astrocytes[45,52]. Such photodamage can be greatly reduced by imaging astrocytes with the lowest laser light intensity possible and in sessions of short duration interspersed with imaging-free periods. In experiments on cultured cells and brain slices, photodamage can be further reduced by adding antioxidants such as L-ascorbate and Trolox (6-hydroxy-2,5,7,8-tetramethylchroman-2-carboxylic acid, a water-soluble analogue of vitamin E) to the culture medium[53,54]. However, antioxidants need to be used with an extreme caution, as high concentrations or prolonged exposure to these agents can directly influence $Ca^{2+}$ signalling[55,56].

***$Ca^{2+}$ buffering.*** $Ca^{2+}$ indicators bind $Ca^{2+}$ and, hence, have an inherent $Ca^{2+}$-buffering effect. This property raises at least two issues that influence the interpretation of indicator-reported $Ca^{2+}$ changes (TABLE 1; BOX 1). First, changes in indicator fluorescence do not directly capture $Ca^{2+}$ dynamics in an unperturbed cell because

these indicators have distinct $Ca^{2+}$ binding and unbinding rates and compete for $Ca^{2+}$ with endogenous $Ca^{2+}$-binding sites in a concentration-dependent manner[47,57,58]. Determining the time course of 'true' $Ca^{2+}$ concentrations is a challenging task that requires precise knowledge of, for instance, all the buffering agents involved, their biophysical properties, their concentrations and the underlying $Ca^{2+}$ signalling mechanisms. Second, the addition of $Ca^{2+}$ indicators could disrupt endogenous signalling mechanisms, in a similar way to the inhibition of $Ca^{2+}$ signalling caused by widely used non-fluorescent $Ca^{2+}$ buffers such as ethylene glycol-bis(2-aminoethyl ether)-*N*,*N*,*N*′,*N*′-tetraacetic acid (EGTA) and 1,2-bis(*o*-aminophenoxy)ethane-*N*,*N*,*N*′,*N*′-tetraacetic acid (BAPTA). Their addition can shield native $Ca^{2+}$-binding sites and also alter the effective diffusion coefficient of $Ca^{2+}$ (REFS[59,60]) in the cytosol, thereby changing its range of action[59,60]. In astrocytes, fluctuations in $Ca^{2+}$ levels can be blunted by the indicators and might not reach the threshold for $Ca^{2+}$-dependent $Ca^{2+}$ release from internal stores such as the endoplasmic reticulum and mitochondria.

Mathematical modelling suggests that exogenous buffers or $Ca^{2+}$ indicators can reduce the amplitude and width of $Ca^{2+}$ events induced by inositol 1,4,5-trisphosphate ($InsP_3$) receptors ($InsP_3Rs$)[59]. This prediction was experimentally confirmed by the loading of cultured astrocytes with low-affinity and high-affinity membrane-permeant $Ca^{2+}$ chelators[61]. Thus, $Ca^{2+}$ indicators can considerably alter the spatio-temporal properties of $Ca^{2+}$ activity in astrocytic networks. Similarly, low-affinity endogenous $Ca^{2+}$ buffers can profoundly shape astrocytic $Ca^{2+}$ signals and their propagation[48,61]. Importantly, the ability of endogenous $Ca^{2+}$ buffers to bind additional $Ca^{2+}$, for instance during $Ca^{2+}$ influx into the astrocyte cytosol, is also influenced by resting $Ca^{2+}$ levels. In turn, resting $Ca^{2+}$ levels determine to what extent endogenous $Ca^{2+}$ buffers are preloaded with $Ca^{2+}$. Detailed information on the identity, concentration and biophysical properties of mobile and immobile $Ca^{2+}$ buffers in astrocytes will be important to obtain in the future.

Imaging $Ca^{2+}$ signals in astrocytes is a favoured method for studying the complex physiology of these cells. Owing to the availability of various viral vectors and transgenic mouse lines[62] carrying GECIs and of two-photon excitation fluorescence microscopy, this versatile method is becoming widely used. Caution in choosing appropriate imaging parameters and awareness of their limitations are required when one is interpreting the biological significance of recorded $Ca^{2+}$ transients.

## Analysing astrocytic $Ca^{2+}$ signals

$Ca^{2+}$ activity within a single astrocyte and in astrocytic networks consists of discrete individual events that emerge at different locations and times. These events differ widely in their amplitude and duration; quite often, neighbouring events can undergo spread and merge into larger events that have distinct spatio-temporal characteristics[18,63,64]. Several concepts, algorithms and methods have been developed to characterize the spatio-temporal patterns of astrocytic $Ca^{2+}$ events. Methods such as single-plane time-lapse fluorescence imaging involve extraction of the total number of active pixels in a time series, whereas other techniques determine the number, sizes and relative positions of individually detected $Ca^{2+}$ events[8,21,45,63–68]. All these methods address different aspects of $Ca^{2+}$ signals. At present, the major challenge is to come up with a robust and physiologically relevant definition of an astrocytic $Ca^{2+}$ event that can be used to design novel, computationally sound and comprehensive analytical tools.

***Detecting astrocytic $Ca^{2+}$ signals.*** Detection of an astrocytic $Ca^{2+}$ signal usually requires the $Ca^{2+}$ level to depart substantially from a fairly well-defined resting value. In common with other types of image processing, setting an appropriate threshold for detection of a $Ca^{2+}$ signal presents a formidable challenge. Among many potential issues, biases can arise from the non-linear transformation of $Ca^{2+}$ concentration transients into fluorescent signals (BOX 1). For instance, when thresholds are applied to data quantified as $\Delta F/F_0$ instead of actual $Ca^{2+}$ concentrations, it is unclear whether $Ca^{2+}$ level increases across the cell and over time have to reach different magnitudes to be detected as events. Thus, threshold selection is non-trivial and can skew the results by including false-positive events as well as by excluding genuine $Ca^{2+}$ events. Multiple-threshold-based and non-threshold-based detection methods could increase the accuracy of event analysis. Indeed, the benefits of multiple-threshold analysis are well known in image segmentation[69] and immunocytochemical studies[70,71]. Such methods could also be useful for the segmentation of $Ca^{2+}$ events in

Box 1 | **$Ca^{2+}$ indicator fluorescence and astrocytic $Ca^{2+}$ concentrations**

Fluorescence intensity reflects the concentration of $Ca^{2+}$-bound $Ca^{2+}$ indicator, which has a non-linear relationship with ambient $Ca^{2+}$ concentrations and experimental factors (including indicator concentration, excitation and fluorescence detection method). Interpretation of the intensity and changes in $Ca^{2+}$ indicator fluorescence is further complicated by the inherent $Ca^{2+}$-buffering capacity of $Ca^{2+}$ indicators, which compete with endogenous molecules for $Ca^{2+}$ binding[47,57,58,143].

Astrocytic $Ca^{2+}$ transients (departures of the $Ca^{2+}$ concentration from the resting level) are often approximated as $\Delta F/F_0$, where $\Delta F$ denotes the change in fluorescence intensity at a given time point relative to the baseline intensity, $F_0$. Such measures account for changes in indicator concentration, excitation and fluorescence collection between experiments and cells, but are easily distorted by movement artefacts (caused by contraction or dilation of blood vessels in contact with astrocyte end-feet and changes in volume or morphology of the astrocyte investigated) that create spurious changes in fluorescence. In addition, organic $Ca^{2+}$ indicators can pass through gap junctions or hemichannels and be sequestered within organelles, thereby lowering their intracellular concentration. Genetically encoded $Ca^{2+}$ indicators also aggregate, accumulate or are sequestered by endogenous proteins[143], which might lead to an undesirable spatial distribution.

$F_0$ depends on both the indicator concentration in the imaged voxel and the resting $Ca^{2+}$ concentration. For astrocytic transients calculated as $\Delta F/F_0$, the same increase in $Ca^{2+}$ concentration appears smaller when the resting $Ca^{2+}$ concentration (and thus $F_0$) is higher in one cellular compartment than in another. Also, for commonly used dyes, $\Delta F$ is decreased for identical $Ca^{2+}$ concentration rises when the resting $Ca^{2+}$ concentration is high. Resting $Ca^{2+}$ concentration can differ substantially between astrocytes and across their subcellular domains[32,44]. Ideally, direct estimates of $Ca^{2+}$ concentrations are obtained with use of calibrated ratiometric dyes (TABLE 1). Alternatively, fluorescence lifetime imaging relies on changes in the fluorescence lifetime of some indicators[144] and has been used successfully to study astrocytic $Ca^{2+}$ signalling[32,43,44,125]. Quantitative two-photon excitation imaging modalities have been reviewed in detail elsewhere[145].

Deconvolution-based techniques
Deconvolution (reversing the inherent image distortion specific to a given microscope or other imaging instrument) is usually done by image-processing software as part of image generation.

Schaffer collaterals
Axon collaterals derived from CA3 pyramidal cells that project to hippocampal area CA1. Schaffer collaterals influence learning and memory via activity-dependent plasticity and are integral to hippocampal medial limbic and trisynaptic circuits.

time-lapse imaging of astrocytes. In addition, individual $Ca^{2+}$ transients could be located by template-matching methods or quantified by deconvolution-based techniques, which have been successfully used to improve the detection of spontaneous synaptic currents[72,73] and $Ca^{2+}$ transients[74,75] in neurons. Finally, frequency-domain analysis (such as spectral or wavelet analysis of overall $Ca^{2+}$ dynamics) might avoid the need to identify distinct astrocytic $Ca^{2+}$ signalling events.

***Region of interest-based analysis.*** Manual or semi-automatic selection of a fixed region of interest (ROI) and the subsequent analysis of time-dependent fluorescence changes in that ROI is a classic method of analysis in all cell types, including astrocytes (FIG. 2a). ROI-based analysis has been successfully used in many preparations, including those in which the initial observations of astrocytic $Ca^{2+}$ signals were made[8,18]. ROI-based analysis is straightforward and easy to implement but has various limitations. First, defining objective criteria for ROI selection is non-trivial, especially in astrocytes with their complex structure and morphology; many astrocyte processes cannot be resolved by diffraction-limited microscopy. Second, the fluorescence intensity of the $Ca^{2+}$ indicator is commonly averaged across the ROI, but this approach results in all information on the spatial structure of the event and its changes within the ROI being lost. This loss is especially problematic for complex astrocytic $Ca^{2+}$ transients, which might develop separately in space and time and merge later, or vice versa (FIG. 2). Therefore, 'smart' ROI-based approaches to automatically identify ROIs have been developed with use of various mathematical models, such as principal component analysis[19,76,77] and machine learning algorithms, including support vector machines[45] (FIG. 2b). Another major problem in automated signal processing is defining the baseline fluorescence value in an ROI. Owing to high variability in the number of $Ca^{2+}$ transients in each ROI, simple mean or median values of these signals cannot be used to normalize the data. A possible solution is to use iterative methods to calculate the absolute mean and standard deviation of the background noise in each ROI, and subsequently to use these values for data normalization in the corresponding ROIs. Both machine learning-based automatic ROI detection and an iterative method for noise calculation in the analysis of astrocyte $Ca^{2+}$ transients have been implemented in a newly developed MATLAB-based algorithm called 'CaSCaDe' (for '$Ca^{2+}$ signal classification and decoding')[45]. Once ROIs have been defined and baseline fluorescence values have been calculated for each ROI, $Ca^{2+}$ activity within these ROIs is analysed with use of standard signal-processing parameters such as the number of active microdomains and the frequency, amplitude or duration of $Ca^{2+}$ transients. However, the activity patterns and characteristics of $Ca^{2+}$ signals within each ROI are complex, and further work is required to refine and develop methods to characterize signals within these ROIs.

***$Ca^{2+}$ event-based analysis.*** As $Ca^{2+}$ events in astrocytes merge, split and propagate in space and time, some events will start and finish outside the boundaries of spatially fixed ROIs (FIG. 2c,d). An increase in the spatial size of $Ca^{2+}$ events could result in their invasion of another nearby fixed ROI, where they will be falsely detected as a new $Ca^{2+}$ transient. The appearance of such false new $Ca^{2+}$ transients has been demonstrated in somatic ROIs in response to bath application of a metabotropic glutamate receptor agonist in cultured astrocytes[21].

The observation that $Ca^{2+}$ events propagate within single astrocytes and through the astrocytic syncytium was first made in cell culture experiments in the 1990s[8,64]. Application of an algorithm for the detection of spatio-temporal $Ca^{2+}$ events in cultured astrocytes[64] showed that the spatial extent of $Ca^{2+}$ events follows a power-law distribution, which suggests that widely used statistics assuming a Gaussian distribution cannot be applied to compare $Ca^{2+}$ event properties. Consistent with this finding in cultured astrocytes[64], a similar algorithm applied to mouse hippocampal slices showed that the size and duration of $Ca^{2+}$ events also followed power-law distributions[21]. In this study, stimulation of Schaffer collaterals increased the spread of $Ca^{2+}$ events detected in the CA1 region, which also changed the power-law exponent.

The detection of spatio-temporal $Ca^{2+}$ events can be used to characterize the patterns of $Ca^{2+}$ activity within the spatial domains of single astrocytes[65,66] in terms of the number of events per frame and the total active area. $Ca^{2+}$ event starting points have also been characterized in relation to astrocyte morphology[67]. Development of the Astrocyte Quantitative Analysis (AQuA) machine learning algorithm led to substantial advances in $Ca^{2+}$ event-based analysis[63]. This algorithm can be used to analyse the propagation path, direction and speed of $Ca^{2+}$ events in different preparations, including in vivo. Importantly, individual $Ca^{2+}$ events in an astrocyte population are associated with a unique pattern of parameters, such as the density of events and their relative positions, sizes and durations (reviewed elsewhere[78]). The links between these patterns and physiological functioning of the astrocytic network are still unclear.

At present, only a few approaches are available to quantify limited aspects of $Ca^{2+}$ activity in astrocytes at the population level, such as measurements of the total active area or the number of $Ca^{2+}$ events per imaging frame[63,65]. The emergence of 3D $Ca^{2+}$ imaging of astrocytes[42] adds another level of complexity and requires the development of sophisticated data-analysis tools to evaluate dynamic changes in the volume and propagation of $Ca^{2+}$ events. No single algorithm is ultimately likely to capture all the diverse activity patterns of $Ca^{2+}$ signals in an astrocyte or an astrocytic network. However, combinations of several complementary analytical methods offer a plausible strategy to extract relevant information for decoding the biological significance of $Ca^{2+}$ transients.

## Interpreting astrocytic $Ca^{2+}$ signals

Neuronal physiology had already been extensively explored with electrophysiological tools before the advent of detailed analysis of astrocytic $Ca^{2+}$ signalling. Therefore, neuronal concepts have often been

applied to astrocytic $Ca^{2+}$ signals for convenience. However, the expression profiles of various channels and receptors suggest that astrocytic signalling operates according to biophysical principles distinct from those in neurons. Hence, the mechanisms that regulate neuronal responses probably cannot be directly extrapolated to astrocytic $Ca^{2+}$ signalling (FIG. 3). Attempts to adapt neuromorphic interpretations and

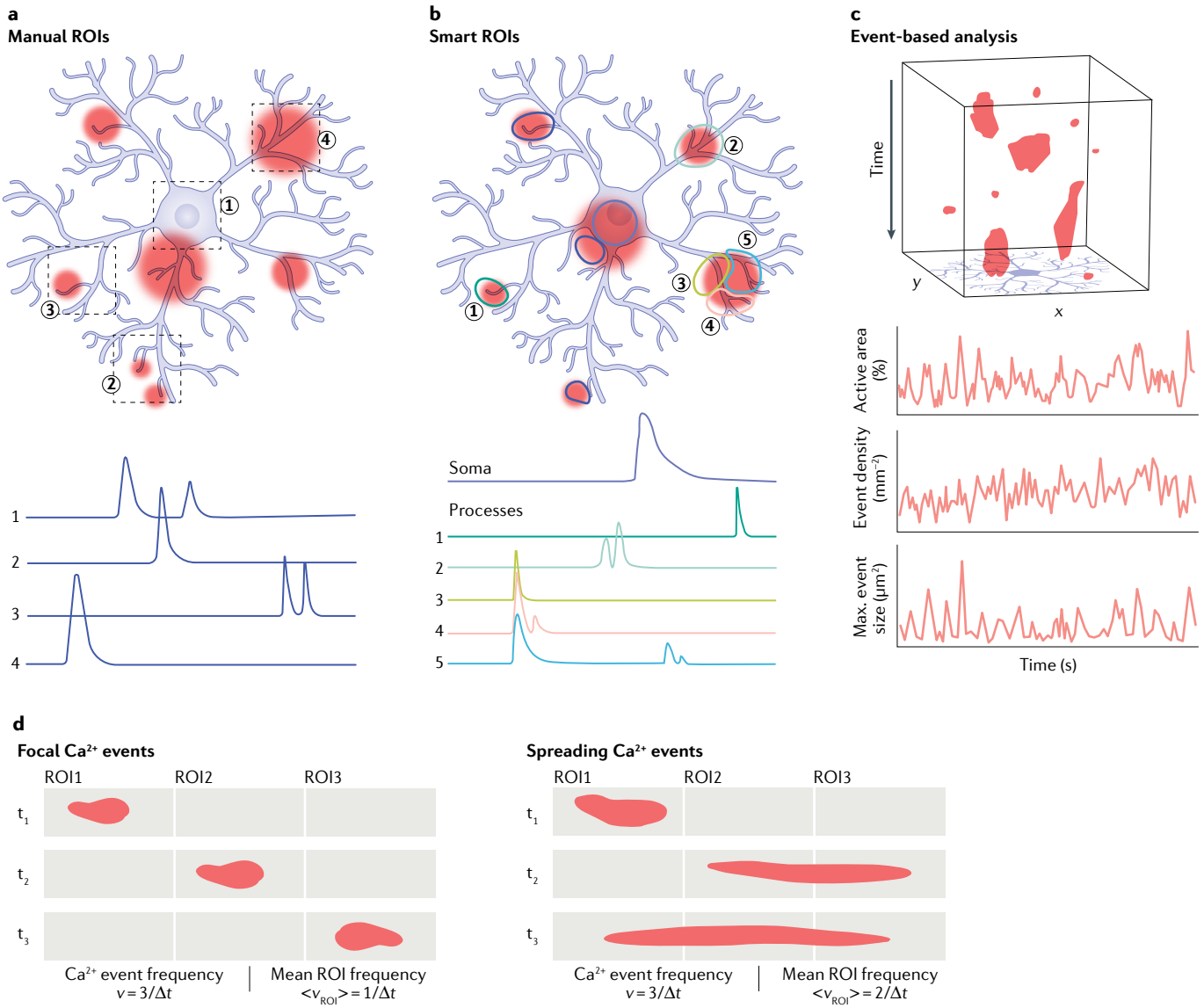


Fig. 2 | **Spatio-temporal analysis of astrocytic $Ca^{2+}$ activity. a** | In manual region of interest (ROI)-based analysis of astrocytic $Ca^{2+}$ signals, ROIs are defined according to visually identified anatomical structures or other criteria without a prior in-depth analysis of $Ca^{2+}$ signals. Therefore, such ROIs might include only parts of spreading events or might contain multiple foci of events within the same frame. When selected ROIs are all the same size (ROIs 1–4), the weight of the pixels in mean fluorescence terms is the same in each ROI. ROIs of differing sizes might also be selected (not shown). The graphs at the bottom show the mean fluorescence intensity from each pixel of ROIs 1–4. **b** | In smart ROI-based analysis of astrocytic $Ca^{2+}$ signals, ROIs are defined with use of mathematical models or machine learning-based algorithms that analyse $Ca^{2+}$ activity in the entire imaging stack and then use various parameters to both select and analyse optimally active regions. These algorithms are designed to adapt to changing levels and distributions of activity across cells and experiments. ROIs can also be determined or refined by astrocyte morphology (such as endoplasmic reticulum tangles or mitochondrial location) and physiology (such as local synaptic activity). As for manual ROIs, $Ca^{2+}$ events in smart ROIs might occupy only part of the frame and might propagate through several adjacent ROIs (see ROIs 3–5). Moreover, smart ROIs have different sizes, and hence different pixel weights contribute to mean fluorescence. The graphs at the bottom show the average of the normalized fluorescence from each pixel of the soma and five selected ROIs. **c** | In event-based analysis, all pixels in which the fluorescence increase exceeds a given threshold are considered active in each recording frame. All adjoining active pixels are considered to be part of a single $Ca^{2+}$ event, and the evolution of this event is traced in subsequent frames. The time course of events in a single astrocyte is shown, with shapes indicating individual $Ca^{2+}$ events. The major drawback of this method is that the spread and duration of $Ca^{2+}$ events strongly depend on the detection threshold selected. The graphs show the time courses of the active area, the density of $Ca^{2+}$ events detected in each frame and the maximal event size. **d** | Limitations of ROI-based analysis are illustrated using an astrocytic process divided into three ROIs at three moments in time ($t_1$, $t_2$, $t_3$). For localized or focal $Ca^{2+}$ signals (left panel), one $Ca^{2+}$ event occurs in each ROI during the recording and event-based imaging analysis records three separate events, whereas ROI-based analysis records one event per ROI. However, when these events expand and propagate (right panel), event-based analysis still reports three separate events, whereas ROIs-based analysis reports multiple events per ROI. Part **d** adapted with permission from REF.[21], Elsevier.

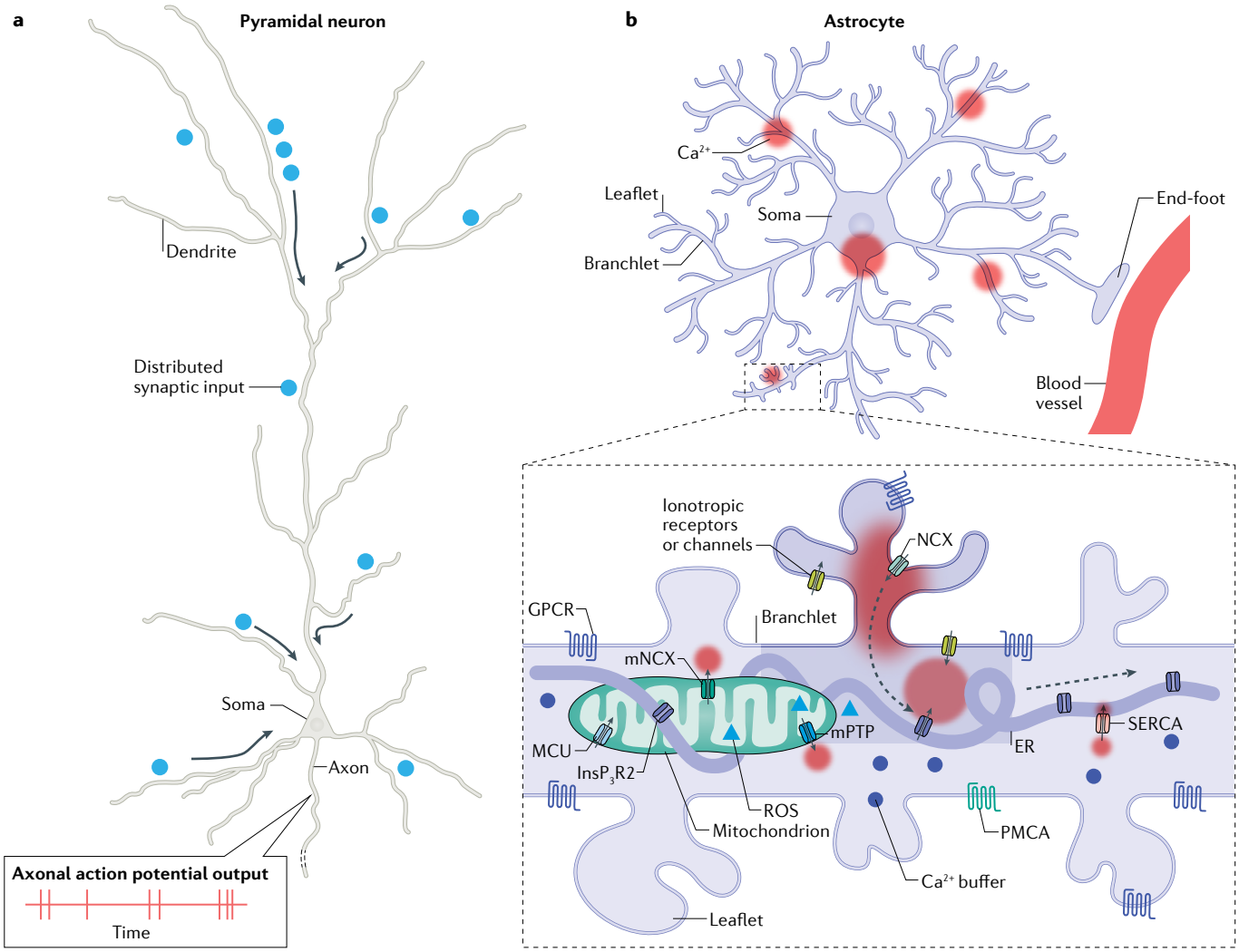


Fig. 3 | **Signal processing in astrocytes and neurons. a** | Simplified information flow in an excitatory neuron such as a pyramidal cell. Spatially and temporally distributed synaptic input is integrated locally in dendritic segments. Dendritic mechanisms determine the flow of electrical signals towards the soma and the axonal hillock, where sequences of action potentials are generated and propagate down the axon to reach their downstream synaptic targets. **b** | In contrast to neurons, the somatic region of astrocytes is not a central signalling hub. Instead, widely distributed foci of $Ca^{2+}$ signals are thought to trigger local downstream signalling cascades that in turn modify local neuronal signalling. Astrocytic processes are categorized as primary branches, higher-order branchlets, terminal leaflets and end-feet that contact blood vessels. Branchlets carry the thin organelle-free leaflets, which are intermingled with neuronal structures and (with a few rare exceptions) do not invade the synaptic cleft. Leaflets generate $Ca^{2+}$ transients owing to $Ca^{2+}$ entry through the plasma membrane (via sodium/calcium exchanger (NCX)) following $Na^{+}$ level elevation during neurotransmitter uptake and other receptors or channels. $Ca^{2+}$ level elevations can propagate into branchlets, which contain endoplasmic reticulum (ER), and can be amplified and propagated by $Ca^{2+}$-dependent $Ca^{2+}$ release through inositol 1,4,5-trisphosphate receptors (IP3Rs). G-protein-coupled receptors (GPCRs) are abundantly expressed by astrocytes and drive astrocytic $Ca^{2+}$ signalling by production of inositol 1,4,5-trisphosphate. In the cytosol, $Ca^{2+}$ is buffered by endogenous buffers and (when they are introduced) $Ca^{2+}$ indicators. Then, $Ca^{2+}$ is removed from the cell by plasma membrane $Ca^{2+}$ ATPase (PCMA) or moved to the ER by sarcoplasmic/endoplasmic reticulum calcium ATPase (SERCA). In addition to ER, astrocytic branchlets contain elongated mitochondria, which actively participate in local $Ca^{2+}$ dynamics by releasing $Ca^{2+}$ through the mitochondrial permeability transition pore (mPTP) and mitochondrial NCX (mNCX) and by sequestering $Ca^{2+}$ via the mitochondrial $Ca^{2+}$ uniporter (MCU). Mitochondria also serve as a source of reactive oxygen species (ROS), which regulate astrocytic $Ca^{2+}$ activity.

neuron-derived concepts to astrocytes are ultimately likely to prove futile.

Astrocytic $Ca^{2+}$ events can be classified as either spontaneous or triggered. Spontaneous $Ca^{2+}$ events are generated intrinsically without any external stimuli, whereas triggered $Ca^{2+}$ events occur in response to changes in the astrocytic environment, such as synaptic or neuronal activity and physiologically relevant internal and external triggers (FIG. 1).

***Spontaneous $Ca^{2+}$ events.*** The precise mechanisms by which spontaneous $Ca^{2+}$ transients are generated in astrocytes remain under investigation. Astrocytes are able to generate spontaneous $Ca^{2+}$ events even when neuronal firing is blocked by tetrodotoxin[79], when neuronal and astrocytic vesicular release is blocked by bafilomycin A1 (REFS[18,80]) and despite genetic knockout of astrocytic $InsP_3R$ type 2 ($InsP_3R2$)[45,77,81]. Most likely, these spontaneous $Ca^{2+}$ events are triggered by stochastic $Ca^{2+}$

fluxes through multiple pathways. $Ca^{2+}$ can enter the cell through $Ca^{2+}$-permeable receptors, $Ca^{2+}$ channels and $Na^+/Ca^{2+}$ exchangers located on the plasma membrane and can pass through $InsP_3Rs$ on the endoplasmic reticulum and through mitochondrial permeability transition pores[17,45,67,78,82,83]. Superposition of these small and spatially restricted $Ca^{2+}$ fluxes leads to local cytosolic fluctuations of $Ca^{2+}$ concentration that can reach the threshold for $Ca^{2+}$-dependent $Ca^{2+}$ release through $InsP_3Rs$, leading to the amplification and propagation of spontaneous $Ca^{2+}$ events[84] (FIGS 3,4).

External stimuli can either modulate existing spontaneous $Ca^{2+}$ activity or trigger new $Ca^{2+}$ responses, although distinguishing between these two scenarios might prove challenging. Glutamate, ATP and noradrenaline can activate the α-subunits of astrocytic $G_q$ proteins ($G_q\alpha$) via the corresponding G-protein-coupled receptors, which leads to the production of diacylglycerol and $InsP_3$ by phospholipase C. The levels of $InsP_3$ and $Ca^{2+}$ jointly determine the open probability of $InsP_3Rs$[85], and a high cytosolic $InsP_3$ concentration increases the chance of spontaneous $Ca^{2+}$ fluctuations becoming amplified through $Ca^{2+}$-dependent $Ca^{2+}$ release. This amplification can convert spatially restricted spontaneous $Ca^{2+}$ events into propagating events, and neuronal activity can thereby boost the propagation of $Ca^{2+}$ events in astrocytes[21]. When $InsP_3R2$ is genetically deleted in mouse astrocytes, spontaneous $Ca^{2+}$ fluctuations (which are mediated by $Ca^{2+}$ entry through the plasma membrane or released by mitochondria) still occur but can no longer be amplified by $Ca^{2+}$-dependent $Ca^{2+}$ release. Hence, the proportion of spreading $Ca^{2+}$ events is greatly decreased in mice lacking $InsP_3R2$ (REFS[45,77,86]).

The stochastic probability of $InsP_3R$ opening and mitochondrial permeability transition pore opening can be further enhanced by increased ROS production[87,88] during states of high metabolic demand, such as increased neuronal firing or enhanced cellular stress during pathological conditions such as epileptic seizures[89], and in astrocytes that overexpress a mutant superoxide dismutase 1 (SOD1) bearing the amino acid substitution Gly93Ala, which leads to the accumulation of cytotoxic levels of intracellular ROS[45]. These studies indicate that ROS can modulate the frequency, spread and duration of spontaneous $Ca^{2+}$ activity in astrocytes. Hence, spontaneous $Ca^{2+}$ transients can be considered to report the internal state of astrocytes. Changes in the characteristics of these transients might act as a sensitive indicator of the metabolic or redox state of the cell.

***Triggered $Ca^{2+}$ events.*** $Ca^{2+}$ events in astrocytes can be triggered by activation of a plethora of cell surface receptors, channels and exchangers. A very common signalling motif is the activation of metabotropic receptors, which increase both cytosolic $InsP_3$ levels and the $InsP_3R$ open probability, thereby promoting $Ca^{2+}$ release from $Ca^{2+}$ stores[1,2]. However, $Ca^{2+}$ can also directly enter the astrocyte cytosol — via, for instance, ionotropic glutamate receptors, purinergic P2X and nicotinic cholinergic receptors — in response to neuronal activity (reviewed elsewhere[2]). In addition, the uptake of glutamate and GABA leads to $Na^+$ influx, which activates $Na^+/Ca^{2+}$ exchangers and can trigger $Ca^{2+}$ transients in astrocytes[90–92]. $G_s\alpha$-coupled and $G_i\alpha$-coupled metabotropic receptors can also trigger $Ca^{2+}$ transients in astrocytes, via an unknown mechanism[62,93]. Astrocytes sense many types of signals, including the volumetric release of neuromodulators and changes in the partial pressures of $CO_2$ and $O_2$, pH, temperature and cerebral perfusion pressure, and often respond to these changes by modulating $Ca^{2+}$ signals[78,94–98].

As a result of the shared intracellular signalling mechanisms involving cytosolic $Ca^{2+}$, $InsP_3$ and $InsP_3Rs$, spontaneously generated $Ca^{2+}$ transients as well as their modulation by receptor activity and receptor-dependent induction of new $Ca^{2+}$ transients are tightly interlinked. Each experimental setting provides a snapshot of this continuum but its specific make-up will depend on many parameters, including neuronal and neuromodulatory activity and metabolic state. This convergence of intracellular signalling mechanisms puts $InsP_3Rs$ at centre stage; astrocytic $Ca^{2+}$ signalling was long thought to depend almost exclusively on $InsP_3R$ signalling. Although $InsP_3R2$ has a major role in astrocytes[99], other $InsP_3Rs$ are also involved[86]. Genetic deletion of $InsP_3Rs$ can be used as a tool to disentangle and isolate $Ca^{2+}$ signalling cascades. In *Ip3r2*$^{-/-}$ mice (*Ip3r2* is also known as *Itpr2*), for instance, very few $Ca^{2+}$ transients are directly triggered by neuronal activity, and most activity represents spontaneous $Ca^{2+}$ transients[45,46,77,100].

***$Ca^{2+}$ activity and astrocyte morphology.*** The amplitude of stochastic $Ca^{2+}$ level fluctuations in astrocytic branchlets depends on their surface-to-volume ratio[68], which is highest in the distal branchlets, where $Ca^{2+}$ entry into the cytosol therefore produces the largest $Ca^{2+}$ level elevations[13,101]. Hence, $Ca^{2+}$ level fluctuations in thin distal branchlets are more likely than somatic $Ca^{2+}$ level fluctuations to reach the threshold for amplification by $Ca^{2+}$-dependent $Ca^{2+}$ release[67]. Quantitative fluorescence lifetime imaging has revealed bigger amplitudes of $Ca^{2+}$ transients in response to metabotropic glutamate receptor agonist treatment in astrocyte regions dominated by distal processes[32]. Several groups have also observed spatial restriction of spontaneous $Ca^{2+}$ events in ex vivo and in vivo preparations[17,45,67,68,81]. These events occur predominantly in distal parts of the astrocyte processes called 'microdomains'[17,45,67,68,81]. Each individual astrocyte possesses a myriad of such microdomains[102]. A study that used stimulated emission depletion microscopy to look for correlations between sub-diffraction-limit astrocyte morphology and subcellular $Ca^{2+}$ activity[103] found that most astrocytic $Ca^{2+}$ transients originate at node-like and synapse-associated structures[103]. Further studies are needed to clarify the ultrastructural composition and molecular make-up of these compartments.

The observation that specific subcellular compartments are privileged with regard to the generation of $Ca^{2+}$ events is intriguing in many ways, not least with regard to the potential relationship between $Ca^{2+}$ dynamics and astrocyte morphology. Morphological remodelling events such as changes in the number of branchlets might regulate $Ca^{2+}$ dynamics[104]. Conversely, $Ca^{2+}$ activity can

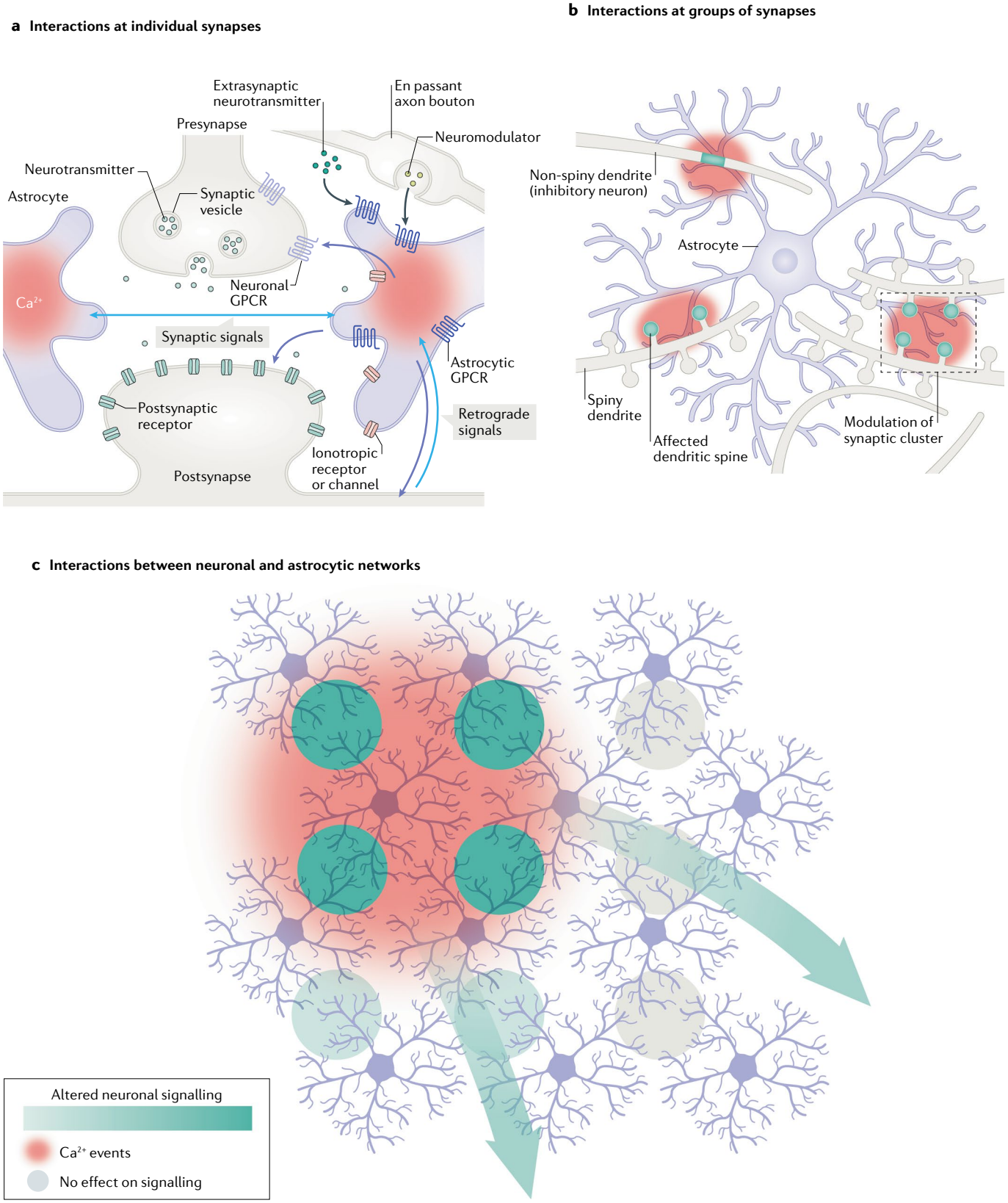


also sculpt astrocyte morphology because $Ca^{2+}$ level rises trigger the outgrowth of peripheral processes through binding of actin to profiline 1 (REF.[105]). Furthermore, expression of an $InsP_3$-absorbing recombinant peptide ($InsP_3$ sponge) reduces activity-dependent modulation of astrocytic $Ca^{2+}$ signals and causes retraction of perisynaptic leaflets in a transgenic mouse model[106]. Hence, neuronal network activity positively modulates

◀ Fig. 4 | **Different levels of interaction between neurons and astrocytes. a** | Synaptic release of neurotransmitters, extrasynaptic neuromodulators such as dopamine and noradrenaline, and retrograde signals such as endocannabinoids trigger $Ca^{2+}$ events in perisynaptic astrocytic leaflets. These $Ca^{2+}$ events induce the release of signalling molecules that affect neuronal excitability, synaptic transmission and plasticity. **b** | $Ca^{2+}$ events within astrocytic microdomains include the territories of multiple synapses and can influence their activity and/or plasticity by releasing signalling molecules or by changing the synaptic microenvironment. This shared exposure leads to the co-modulation of multiple synapses (synaptic clusters) both on the same and on different dendrites and/or neurons. **c** | $Ca^{2+}$ events (waves) spread through astrocytes and the astrocytic network and change the state of groups of neurons, thereby guiding information processing across the neuronal network. GPCR, G-protein-coupled receptor.

astrocytic $Ca^{2+}$ signalling, and the reduction of neuronal activity can lead to the retraction of astrocytic leaflets. This interplay between neuronal activity and astrocyte structural changes ultimately reaches an equilibrium that ensures the optimal operation of an astrocyte–neuron network.

***Speed of astrocytic $Ca^{2+}$ signalling.*** Neuronal activity, as opposed to non-neuronal brain processes, is often solely linked to real-time information processing in the brain (examples of which include place cell activity, rate coding and neuronal firing locked to the phase of brain rhythms)[107–109]. Astrocytic $Ca^{2+}$ signalling is considered too slow to be involved in real-time information processing. Indeed, a single action potential in a neuron lasts a few milliseconds and postsynaptic potentials last a few tens of milliseconds, whereas astrocytic $Ca^{2+}$ events occur over durations of several hundred milliseconds to a few seconds. In addition, astrocytic $Ca^{2+}$ signalling is characterized by large jitter, meaning that astrocytic responses to external stimulation or neuronal activity might be considerably delayed. The mean interval between sensory stimulation and onset of an astrocytic $Ca^{2+}$ event is highly variable (range 1.0–5.5 s)[31,46,110]. Nonetheless, a small subset (~8%) of astrocytic $Ca^{2+}$ events are 'fast' events, which have a mean onset time of ~333 ms, as rapid as that of some neurons (neuronal mean onset time ~208 ms)[46,111]. On average, an astrocyte microdomain experiences 0.5–1.0 $Ca^{2+}$ transients per minute during baseline activity, and this rate can rise to 5–10 $Ca^{2+}$ transients per minute during stimulation[42,45]. Therefore, an individual astrocyte can sense a diverse range of neuronal signals and integrate this information to derive an appropriate response, which can be simultaneously 'fast' and 'slow' at distinct locations of the cell.

The human reaction time to visual and auditory stimuli is ~100 ms (REFS[112,113]), whereas responding to the conscious intention to move takes more than 1 s (REF.[114]). Neurons can generate meaningful sequences of tens to hundreds of action potentials in such time spans. Astrocytic $Ca^{2+}$ events might therefore be too slow for rate-based information encoding. However, astrocytes could also encode information in patterns of $Ca^{2+}$ events. Imaging data show that astrocytic $Ca^{2+}$ activity patterns (that is, the total area, number and duration of $Ca^{2+}$ events) change in each imaging frame[63,65]. Indeed, some $Ca^{2+}$ events start and others end at any given moment in time. As a result, spatial patterns of astrocytic activity can change almost instantaneously (FIG. 2).

$InsP_3$ sponge
A recombinant peptide including modified ligand-binding domains from mouse inositol 1,4,5-trisphosphate ($IP_3$) receptor type 1 ($IP_3R1$), designed to sequester intracellular $InsP_3$ owing to its ~1,000-fold higher affinity for $InsP_3$ than for native IP3Rs.

APP/PS1 mice
A double-transgenic mouse model of Alzheimer disease that expresses both chimeric (mouse–human) amyloid precursor protein (APP) and mutant human presenilin 1 (PS1) specifically in CNS neurons.

***$Ca^{2+}$ signalling in astrocytic networks.*** Individual astrocytes are coupled to their neighbours via gap junctions to form large-scale networks. Gap junctions are permeable to small molecules, including $Ca^{2+}$, $InsP_3$ and ROS, a characteristic that has long been considered to enable $Ca^{2+}$ signals to propagate through the network. Indeed, an early discovery in cultured astrocytes was that intercellular $Ca^{2+}$ waves are sensitive to gap junction blockade[115]. Furthermore, although connexins are closed by high concentrations of $Ca^{2+}$ (such as are found in the extracellular space)[116], intracellular $Ca^{2+}$ waves can be mediated by $InsP_3$ diffusion through gap junctions[117]. In addition to gap junctions, astrocytes communicate with each other through vesicular and non-vesicular release of gliotransmitters such as ATP, glutamate and D-serine[3]. Astrocytic ATP release is also implicated in the propagation of $Ca^{2+}$ activity in cultured astrocytic networks[118], although no intercellular $Ca^{2+}$ waves have been detected in brain slices[20]. Nevertheless, simultaneous $Ca^{2+}$ transients have been observed in multiple astrocytes in vivo during locomotion[28,31,81], in response to visual[30,119] or whisker[46] stimulation and in APP/PS1 mice[43]. However, $Ca^{2+}$ signals could falsely seem to travel in a wave-like manner through an astrocytic network when $Ca^{2+}$ transients are separately but sequentially triggered in different cells, for example by neuromodulators or spreading neuronal activity (such as spreading depression or epilepsy)[31,120].

***Effect of neuromodulators.*** A neuromodulator is a molecule that is not classed as a fast synaptic neurotransmitter but nonetheless affects the excitability and/or firing rate of a population of neurons, a sometimes ambiguous distinction. Classic neuromodulators such as noradrenaline, dopamine, acetylcholine and serotonin are released throughout the brain and spinal cord from subcortical projections located in distinct nuclei. However, such direct neuron-to-neuron neuromodulation is complemented by emerging findings that neuromodulators can also target astrocytes and influence $Ca^{2+}$ activity in astrocytic networks across brain regions and species[4,5,121–123]. Noradrenaline, in particular, can modulate the $Ca^{2+}$ activity of astrocytic networks and enable them to respond to local changes in neuronal activity[29,31,119,124]. For example, in zebrafish, repetitive noradrenaline-mediated $Ca^{2+}$ signals in astrocytes lead to activation of downstream neurons and suppression of futile behaviour[5]. In *Drosophila*, noradrenaline-like neuromodulators such as tyramine and octopamine directly activate astrocytes, which in turn modulate downstream dopaminergic neurons and alter complex behaviours such as olfactory-driven chemotaxis and the touch-induced startle response[4]. Similarly, in rodents, a transient increase in noradrenaline in response to whisker stimulation resulted in a transient $Ca^{2+}$ rise in astrocytes, whereas repetition of an aversive stimulus led to sustained adrenergic release resulting in increased levels of intracellular $Ca^{2+}$ and cAMP in a large population of astrocytes[124]. The neuromodulators dopamine and acetylcholine can also trigger or modify astrocytic $Ca^{2+}$ signals. For instance, dopamine can induce dose-dependent and bidirectional astrocytic $Ca^{2+}$ responses in

the hippocampus[125] and nucleus accumbens[126]. Similarly, acetylcholine can induce $Ca^{2+}$ transients in cortical and hippocampal astrocytes that modulate synaptic transmission and synaptic plasticity[121,127]. In general, astrocytic responses increase the number of possible local effects of a single neuromodulator, and the net effect is likely to differ between different brain regions and according to behavioural context. In turn, the physiological or pathophysiological remodelling of astrocytes, with respect to their ability to sense neuromodulators, integrate this input and modify neuronal signalling, might profoundly alter the local effect of a neuromodulator. Thus, by integrating the information carried by neuromodulators, astrocytes act as potent and rapid regulators of behavioural states.

Neurons influence astrocytic $Ca^{2+}$ activity via two pathways: local interactions at the level of individual synapses and volume transmission through the diffuse release of neuromodulators. Both pathways change the spatio-temporal properties of spontaneous $Ca^{2+}$ events and trigger new $Ca^{2+}$ events. These observations raise several important questions: does a specific pattern of $Ca^{2+}$ events underlie the activation of astrocytes embedded in neural circuits? If such a pattern exists, what information could be encoded by the activation of ensembles of astrocytes and/or astrocyte subregions, and how do they specifically affect neural network activity? (See FIG. 4.)

## Conclusions

Advances in imaging technologies have driven a corresponding increase in the complexity of experimental preparations for studying astrocytic $Ca^{2+}$ events, from cultured cells and brain slices towards imaging in freely moving animals and 3D methods for imaging $Ca^{2+}$ events (although 3D approaches have not yet been widely adopted). ROI-based and event-based data analysis offer complementary approaches for the detection and analysis of spatio-temporal $Ca^{2+}$ signals. Such multifaceted characterization of the spatio-temporal properties of $Ca^{2+}$ events is expected to enable researchers to identify the most physiologically relevant event characteristics — for example, those specifically associated with sensory input, behavioural output, patterns of neuronal network activity or wakefulness.

For example, despite the much slower time course of astrocytic $Ca^{2+}$ signals compared with neuronal electrical signals, population activity in the astrocytic network as a whole can change very quickly, and hence astrocytes could potentially participate in real-time coding of information in the brain. $Ca^{2+}$ signalling in individual astrocytes and astrocytic networks is now known to be intimately linked to astrocyte morphology and to the spatial distribution of the cellular and subcellular components that shape $Ca^{2+}$ signals. However, $Ca^{2+}$-dependent morphological interactions between neurons and astrocytes need to be further investigated, especially in in vivo models. Until the development of super-resolution microscopy, in vivo morphological studies of astrocytes were subject to diffraction-limited optical imaging, which fails to resolve fine astrocytic processes. Astrocyte morphology studies using super-resolution microscopy in combination with simultaneous $Ca^{2+}$ imaging can potentially close this knowledge gap.

Further studies will also be essential to identify links between the appearance of specific astrocytic $Ca^{2+}$ patterns (such as 'place patterns') and animal behaviour, location in space, emotional state and memory acquisition. Indeed, the fact that external stimuli and behaviours can robustly trigger astroglial $Ca^{2+}$ signalling raises several important questions: can defined levels of neuronal activity summon specific $Ca^{2+}$ patterns in astrocytes? Can learning produce long-term changes in astrocytic $Ca^{2+}$ patterns, for example through the morphological and functional plasticity of astrocytes? Can the reproduction of specific astrocytic $Ca^{2+}$ patterns with optogenetic tools result in either the recall of corresponding memories or the triggering of corresponding behaviours? Astrocytic $Ca^{2+}$ activity patterns could therefore represent a guiding template that modifies the state of the local neuronal network, an intriguing possibility suggesting that the information-possessing capacity of the mammalian brain is considerably larger than we currently acknowledge.

Published online 1 September 2020


1. Bazargani, N. & Attwell, D. Astrocyte calcium signaling: the third wave. *Nat. Neurosci.* **19**, 182–189 (2016).
2. Verkhratsky, A. & Nedergaard, M. Physiology of astroglia. *Physiol. Rev.* **98**, 239–389 (2018).
3. Araque, A. et al. Gliotransmitters travel in time and space. *Neuron* **81**, 728–739 (2014).
4. Ma, Z., Stork, T., Bergles, D. E. & Freeman, M. R. Neuromodulators signal through astrocytes to alter neural circuit activity and behaviour. *Nature* **539**, 428–432 (2016).
5. Mu, Y. et al. Glia accumulate evidence that actions are futile and suppress unsuccessful behavior. *Cell* **178**, 27–43 (2019).
**This and the study by Ma et al. (2016) elegantly show in *Drosophila* and zebrafish models that astrocytic $Ca^{2+}$ transients follow similar rules and respond to the same set of neuromodulatory signals as those described in rodents to modify behaviour.**
6. Schummers, J., Yu, H. & Sur, M. Tuned responses of astrocytes and their influence on hemodynamic signals in the visual cortex. *Science* **320**, 1638–1643 (2008).
7. Navarrete, M. et al. Astrocyte calcium signal and gliotransmission in human brain tissue. *Cereb. Cortex* **23**, 1240–1246 (2013).
8. Cornell-Bell, A., Finkbeiner, S., Cooper, M. & Smith, S. Glutamate induces calcium waves in cultured astrocytes: long-range glial signaling. *Science* **247**, 470–473 (1990).
**Pioneering observation of spontaneous astrocytic $Ca^{2+}$ signals demonstrating that astrocytes react to the neurotransmitter glutamate.**
9. Shigetomi, E., Kracun, S., Sofroniew, M. V. & Khakh, B. S. A genetically targeted optical sensor to monitor calcium signals in astrocyte processes. *Nat. Neurosci.* **13**, 759–766 (2010).
10. Lange, S. C., Bak, L. K., Waagepetersen, H. S., Schousboe, A. & Norenberg, M. D. Primary cultures of astrocytes: their value in understanding astrocytes in health and disease. *Neurochem. Res.* **37**, 2569–2588 (2012).
11. Carmignoto, G., Pasti, L. & Pozzan, T. On the role of voltage-dependent calcium channels in calcium signaling of astrocytes in situ. *J. Neurosci.* **18**, 4637–4645 (1998).
12. Foo, L. C. et al. Development of a method for the purification and culture of rodent astrocytes. *Neuron* **71**, 799–811 (2011).
13. Gavrilov, N. et al. Astrocytic coverage of dendritic spines, dendritic shafts, and axonal boutons in hippocampal neuropil. *Front. Cell. Neurosci.* https://doi.org/10.3389/fncel.2018.00248 (2018).
14. Khakh, B. S. & Sofroniew, M. V. Diversity of astrocyte functions and phenotypes in neural circuits. *Nat. Neurosci.* **18**, 942–952 (2015).
15. Mulligan, S. J. & MacVicar, B. A. Calcium transients in astrocyte endfeet cause cerebrovascular constrictions. *Nature* **431**, 195–199 (2004).
16. Medvedev, N. et al. Glia selectively approach synapses on thin dendritic spines. *Philos. Trans. R. Soc. Lond. B Biol. Sci.* **369**, 20140047 (2014).
17. Rungta, R. L. et al. $Ca^{2+}$ transients in astrocyte fine processes occur via $Ca^{2+}$ influx in the adult mouse hippocampus. *Glia* **64**, 2093–2103 (2016).
18. Nett, W. J., Oloff, S. H. & McCarthy, K. D. Hippocampal astrocytes in situ exhibit calcium oscillations that occur independent of neuronal activity. *J. Neurophysiol.* **87**, 528–537 (2002).
19. Di Castro, M. A. et al. Local $Ca^{2+}$ detection and modulation of synaptic release by astrocytes. *Nat. Neurosci.* **14**, 1276–1284 (2011).
20. Porter, J. T. & McCarthy, K. D. Hippocampal astrocytes in situ respond to glutamate released from synaptic terminals. *J. Neurosci.* **16**, 5073–5081 (1996).
**One of the first observations in hippocampal slices showing that synaptic activity leads to astrocytic $Ca^{2+}$ signals.**

21. Wu, Y.-W. et al. Spatiotemporal calcium dynamics in single astrocytes and its modulation by neuronal activity. *Cell Calcium* **55**, 119–129 (2014).
**These authors analyse the spatio-temporal properties of $Ca^{2+}$ events in hippocampal slices and demonstrate that neuronal stimulation modulates their properties (for example, spread) rather than triggers new events**.
22. Pasti, L., Volterra, A., Pozzan, T. & Carmignoto, G. Intracellular calcium oscillations in astrocytes: a highly plastic, bidirectional form of communication between neurons and astrocytes in situ. *J. Neurosci.* **17**, 7817–7830 (1997).
23. Navarrete, M. & Araque, A. Endocannabinoids mediate neuron-astrocyte communication. *Neuron* **57**, 883–893 (2008).
24. Takano, T. et al. Rapid manifestation of reactive astrogliosis in acute hippocampal brain slices. *Glia* **62**, 78–95 (2014).
25. Hirase, H., Qian, L., Bartho, P. & Buzsaki, G. Calcium dynamics of cortical astrocytic networks in vivo. *PLoS Biol.* **2**, E96 (2004).
**Pioneering work showing recordings of astrocytic $Ca^{2+}$ activity in vivo. The authors demonstrate that increased neuronal discharges are associated with increased astrocytic $Ca^{2+}$ activity in individual cells**.
26. Wang, X. et al. Astrocytic $Ca^{2+}$ signaling evoked by sensory stimulation in vivo. *Nat. Neurosci.* **9**, 816–823 (2006).
27. Thrane, A. S. et al. General anesthesia selectively disrupts astrocyte calcium signaling in the awake mouse cortex. *Proc. Natl Acad. Sci. USA* **109**, 18974–18979 (2012).
**This study uses two-photon imaging in vivo to show that the use of anaesthetics blocks $Ca^{2+}$ transients in astrocytes**.
28. Dombeck, D. A., Khabbaz, A. N., Collman, F., Adelman, T. L. & Tank, D. W. Imaging large-scale neural activity with cellular resolution in awake, mobile mice. *Neuron* **56**, 43–57 (2007).
**This work demonstrates an association between mouse running and astrocytic $Ca^{2+}$ signals**.
29. Ding, F. et al. α1-Adrenergic receptors mediate coordinated $Ca^{2+}$ signaling of cortical astrocytes in awake, behaving mice. *Cell Calcium* **54**, 387–394 (2013).
30. Sonoda, K., Matsui, T., Bito, H. & Ohki, K. Astrocytes in the mouse visual cortex reliably respond to visual stimulation. *Biochem. Biophys. Res. Commun.* **505**, 1216–1222 (2018).
31. Paukert, M. et al. Norepinephrine controls astroglial responsiveness to local circuit activity. *Neuron* **82**, 1263–1270 (2014).
32. King, C. M. et al. Local resting $Ca^{2+}$ controls the scale of astroglial $Ca^{2+}$ signals. *Cell Rep.* **30**, 3466–3477 (2020).
**This quantitative $Ca^{2+}$ imaging study reveals that the local resting $Ca^{2+}$ level dynamically controls the magnitude of astrocytic $Ca^{2+}$ transients in both acute brain slices and awake mice**.
33. Kislin, M. et al. Flat-floored air-lifted platform: a new method for combining behavior with microscopy or electrophysiology on awake freely moving rodents. *J. Vis. Exp.* https://doi.org/10.3791/51869 (2014).
34. Royer, S. et al. Control of timing, rate and bursts of hippocampal place cells by dendritic and somatic inhibition. *Nat. Neurosci.* **15**, 769–775 (2012).
35. Thurley, K. & Ayaz, A. Virtual reality systems for rodents. *Curr. Zool.* **63**, 109–119 (2016).
36. Yang, G., Pan, F., Parkhurst, C. N., Grutzendler, J. & Gan, W.-B. Thinned-skull cranial window technique for long-term imaging of the cortex in live mice. *Nat. Protoc.* **5**, 201–208 (2010).
37. Vasile, F., Dossi, E. & Rouach, N. Human astrocytes: structure and functions in the healthy brain. *Brain Struct. Funct.* **222**, 2017–2029 (2017).
38. Oberheim, N. A. et al. Uniquely hominid features of adult human astrocytes. *J. Neurosci.* **29**, 3276–3287 (2009).
39. Bedner, P., Jabs, R. & Steinhäuser, C. Properties of human astrocytes and NG2 glia. *Glia* **68**, 756–767 (2020).
40. Paşca, A. M. et al. Functional cortical neurons and astrocytes from human pluripotent stem cells in 3D culture. *Nat. Methods* **12**, 671–678 (2015).
41. Hansen, M. G., Tornero, D., Canals, I., Ahlenius, H. & Kokaia, Z. in *Neural Stem Cells: Methods and Protocols* (ed. Daadi M. M.) 73–88 (Springer, 2019).
42. Bindocci, E. et al. Three-dimensional $Ca^{2+}$ imaging advances understanding of astrocyte biology. *Science* https://doi.org/10.1126/science.aai8185 (2017).
**These authors propose the use of 3D imaging to monitor $Ca^{2+}$ activity**.
43. Kuchibhotla, K. V., Lattarulo, C. R., Hyman, B. T. & Bacskai, B. J. Synchronous hyperactivity and intercellular calcium waves in astrocytes in Alzheimer mice. *Science* **323**, 1211–1215 (2009).
44. Zheng, K. et al. Time-resolved imaging reveals heterogeneous landscapes of nanomolar $Ca^{2+}$ in neurons and astroglia. *Neuron* **88**, 277–288 (2015).
45. Agarwal, A. et al. Transient opening of the mitochondrial permeability transition pore induces microdomain calcium transients in astrocyte processes. *Neuron* **93**, 587–605 e587 (2017).
**This study shows that mitochondria are involved in $Ca^{2+}$ release and uptake at astrocyte microdomains and that cellular stress increases microdomain $Ca^{2+}$ transients. The authors develop a smart-ROI-based and machine learning-based algorithm (CaSCaDe) for the analysis of $Ca^{2+}$ signals in astrocytes**.
46. Stobart, J. L. et al. Cortical circuit activity evokes rapid astrocyte calcium signals on a similar timescale to neurons. *Neuron* **98**, 726–735 e724 (2018).
47. Sabatini, B. L. & Regehr, W. G. Optical measurement of presynaptic calcium currents. *Biophys. J.* **74**, 1549–1563 (1998).
48. Savtchenko, L. P. et al. Disentangling astroglial physiology with a realistic cell model in silico. *Nat. Commun.* **9**, 3554 (2018).
49. Kuga, N., Sasaki, T., Takahara, Y., Matsuki, N. & Ikegaya, Y. Large-scale calcium waves traveling through astrocytic networks in vivo. *J. Neurosci.* **31**, 2607–2614 (2011).
50. Shibasaki, K., Ikenaka, K., Tamalu, F., Tominaga, M. & Ishizaki, Y. A novel subtype of astrocytes expressing TRPV4 (transient receptor potential vanilloid 4) regulates neuronal excitability via release of gliotransmitters. *J. Biol. Chem.* **289**, 14470–14480 (2014).
51. Dunn, K. M., Hill-Eubanks, D. C., Liedtke, W. B. & Nelson, M. T. TRPV4 channels stimulate $Ca^{2+}$ release in astrocytic endfeet and amplify neurovascular coupling responses. *Proc. Natl Acad. Sci. USA* **110**, 6157–6162 (2013).
52. Jacobson, J. & Duchen, M. R. Mitochondrial oxidative stress and cell death in astrocytes — requirement for stored $Ca^{2+}$ and sustained opening of the permeability transition pore. *J. Cell Sci.* **115**, 1175–1188 (2002).
53. Sacconi, L., Dombeck, D. A. & Webb, W. W. Overcoming photodamage in second-harmonic generation microscopy: real-time optical recording of neuronal action potentials. *Proc. Natl Acad. Sci. USA* **103**, 3124–3129 (2006).
54. Knight, M. M., Roberts, S. R., Lee, D. A. & Bader, D. L. Live cell imaging using confocal microscopy induces intracellular calcium transients and cell death. *Am. J. Physiol. Cell Physiol.* **284**, C1083–C1089 (2003).
55. Freitas, H. R. et al. Glutathione-induced calcium shifts in chick retinal glial cells. *PLoS ONE* **11**, e0153677 (2016).
56. Martinovich, G. G., Golubeva, E. N., Martinovich, I. V. & Cherenkevich, S. N. Redox regulation of calcium signaling in cancer cells by ascorbic acid involving the mitochondrial electron transport chain. *J. Biophys.* **2012**, 921653 (2012).
57. Neher, E. & Augustine, G. J. Calcium gradients and buffers in bovine chromaffin cells. *J. Physiol.* **450**, 273–301 (1992).
58. McMahon, S. M. & Jackson, M. B. An inconvenient truth: calcium sensors are calcium buffers. *Trends Neurosci.* **41**, 880–884 (2018).
59. Jafri, M. S. & Keizer, J. On the roles of $Ca^{2+}$ diffusion, $Ca^{2+}$ buffers, and the endoplasmic reticulum in IP3-induced $Ca^{2+}$ waves. *Biophys. J.* **69**, 2139–2153 (1995).
60. Matthews, E. A. & Dietrich, D. Buffer mobility and the regulation of neuronal calcium domains. *Front. Cell. Neurosci.* https://doi.org/10.3389/fncel.2015.00048 (2015).
61. Wang, Z., Tymianski, M., Jones, O. T. & Nedergaard, M. Impact of cytoplasmic calcium buffering on the spatial and temporal characteristics of intercellular calcium signals in astrocytes. *J. Neurosci.* **17**, 7359–7371 (1997).
62. Yu, X., Nagai, J. & Khakh, B. S. Improved tools to study astrocytes. *Nat. Rev. Neurosci.* **21**, 121–138 (2020).
63. Wang, Y. et al. Accurate quantification of astrocyte and neurotransmitter fluorescence dynamics for single-cell and population-level physiology. *Nat. Neurosci.* **22**, 1936–1944 (2019).
**These authors further improve the method of detection of spatio-temporal $Ca^{2+}$ events in astrocytes and suggest a measure of event propagation path, direction and speed**.
64. Jung, P., Cornell-Bell, A., Madden, K. S. & Moss, F. Noise-induced spiral waves in astrocyte syncytia show evidence of self-organized criticality. *J. Neurophysiol.* **79**, 1098–1101 (1998).
**These authors suggest a new method for quantitatively measuring the spatio-temporal extent of $Ca^{2+}$ waves in cultured astrocytes. They report a power-law distribution of wave sizes, which is characteristic of self-organized critical phenomena**.
65. Nakayama, R., Sasaki, T., Tanaka, K. F. & Ikegaya, Y. Subcellular calcium dynamics during juvenile development in mouse hippocampal astrocytes. *Eur. J. Neurosci.* **43**, 923–932 (2016).
**These authors examine developmental changes in the spatio-temporal patterns of $Ca^{2+}$ activity in single hippocampal astrocytes**.
66. Asada, A. et al. Subtle modulation of ongoing calcium dynamics in astrocytic microdomains by sensory inputs. *Physiol. Rep.* https://doi.org/10.14814/phy2.12454 (2015).
67. Wu, Y.-W. et al. Morphological profile determines the frequency of spontaneous calcium events in astrocytic processes. *Glia* **67**, 246–262 (2019).
68. Stobart, J. L. et al. Long-term in vivo calcium imaging of astrocytes reveals distinct cellular compartment responses to sensory stimulation. *Cereb. Cortex* **28**, 184–198 (2018).
69. Kittler, J. & Illingworth, J. Minimum error thresholding. *Pattern Recognit.* **19**, 41–47 (1986).
70. Stevens, B. et al. The classical complement cascade mediates CNS synapse elimination. *Cell* **131**, 1164–1178 (2007).
71. Torborg, C. L. & Feller, M. B. Unbiased analysis of bulk axonal segregation patterns. *J. Neurosci. Methods* **135**, 17–26 (2004).
72. Clements, J. D. & Bekkers, J. M. Detection of spontaneous synaptic events with an optimally scaled template. *Biophys. J.* **73**, 220–229 (1997).
73. Pernía-Andrade, A. J. et al. A deconvolution-based method with high sensitivity and temporal resolution for detection of spontaneous synaptic currents in vitro and in vivo. *Biophys. J.* **103**, 1429–1439 (2012).
74. Friedrich, J., Zhou, P. & Paninski, L. Fast online deconvolution of calcium imaging data. *PLoS Comput. Biol.* **13**, e1005423 (2017).
75. Szymanska, A. F. et al. Accurate detection of low signal-to-noise ratio neuronal calcium transient waves using a matched filter. *J. Neurosci. Methods* **259**, 1–12 (2016).
76. Mukamel, E. A., Nimmerjahn, A. & Schnitzer, M. J. Automated analysis of cellular signals from large-scale calcium imaging data. *Neuron* **63**, 747–760 (2009).
77. Srinivasan, R. et al. $Ca^{2+}$ signaling in astrocytes from $IP3R2^{-/-}$ mice in brain slices and during startle responses in vivo. *Nat. Neurosci.* **18**, 708–717 (2015).
78. Semyanov, A. Spatiotemporal pattern of calcium activity in astrocytic network. *Cell Calcium* **78**, 15–25 (2019).
79. Wang, T.-f., Zhou, C., Tang, A.-h., Wang, S.-q. & Chai, Z. Cellular mechanism for spontaneous calcium oscillations in astrocytes. *Acta Pharmacol. Sin.* **27**, 861–868 (2006).
80. Sun, M. Y. et al. Astrocyte calcium microdomains are inhibited by bafilomycin A1 and cannot be replicated by low-level Schaffer collateral stimulation in situ. *Cell Calcium* **55**, 1–16 (2014).
81. Bojarskaite, L. et al. Astrocytic $Ca^{2+}$ signaling is reduced during sleep and is involved in the regulation of slow wave sleep. *Nat. Commun.* **11**, 3240 (2020).
82. Denizot, A., Arizono, M., Nägerl, U. V., Soula, H. & Berry, H. Simulation of calcium signaling in fine astrocytic processes: Effect of spatial properties on spontaneous activity. *PLoS Comput. Biol.* **15**, e1006795 (2019).
83. Parri, H. R., Gould, T. M. & Crunelli, V. Spontaneous astrocytic $Ca^{2+}$ oscillations in situ drive NMDAR-mediated neuronal excitation. *Nat. Neurosci.* **4**, 803–812 (2001).
84. Khakh, B. S. & McCarthy, K. D. Astrocyte calcium signaling: from observations to functions and the challenges therein. *Cold Spring Harb. Perspect. Biol.* **7**, a020404 (2015).
85. Foskett, J. K., White, C., Cheung, K.-H. & Mak, D.-O. D. Inositol trisphosphate receptor $Ca^{2+}$ release channels. *Physiol. Rev.* **87**, 593–658 (2007).
86. Sherwood, M. W. et al. Astrocytic IP3Rs: contribution to $Ca^{2+}$ signalling and hippocampal LTP. *Glia* **65**, 502–513 (2017).
87. Wang, W. et al. Superoxide flashes in single mitochondria. *Cell* **134**, 279–290 (2008).
88. Bánsághi, S. et al. Isoform- and species-specific control of inositol 1,4,5-trisphosphate (IP3) receptors by

reactive oxygen species. *J. Biol. Chem.* **289**, 8170–8181 (2014).
89. Faust, T. E. et al. Astrocyte redox dysregulation causes prefrontal hypoactivity: sulforaphane treats non-ictal pathophysiology in ALDH7A1-mediated epilepsy. *bioRxiv* https://doi.org/10.1101/796474 (2019).
90. Boddum, K. et al. Astrocytic GABA transporter activity modulates excitatory neurotransmission. *Nat. Commun.* **7**, 13572 (2016).
91. Rose, C. R., Ziemens, D. & Verkhratsky, A. On the special role of NCX in astrocytes: translating $Na^+$ transients into intracellular $Ca^{2+}$ signals. *Cell Calcium* **86**, 102154 (2020).
92. Brazhe, A. R., Verisokin, A. Y., Verveyko, D. V. & Postnov, D. E. Sodium–calcium exchanger can account for regenerative $Ca^{2+}$ entry in thin astrocyte processes. *Front. Cell. Neurosci.* https://doi.org/10.3389/fncel.2018.00250 (2018).
93. Durkee, C. A. et al. Gi/o protein-coupled receptors inhibit neurons but activate astrocytes and stimulate gliotransmission. *Glia* **67**, 1076–1093 (2019).
94. Turovsky, E. et al. Mechanisms of $CO_2$/$H^+$ sensitivity of astrocytes. *J. Neurosci.* **36**, 10750–10758 (2016).
95. Angelova, P. R. et al. Functional oxygen sensitivity of astrocytes. *J. Neurosci.* **35**, 10460–10473 (2015).
96. Tran, C. H. T., Peringod, G. & Gordon, G. R. Astrocytes integrate behavioral state and vascular signals during functional hyperemia. *Neuron* **100**, 1133–1148 (2018).
97. Marina, N. et al. Astrocytes monitor cerebral perfusion and control systemic circulation to maintain brain blood flow. *Nat. Commun.* **11**, 131 (2020).
98. Ma, Z. & Freeman, M. R. TrpML-mediated astrocyte microdomain $Ca^{2+}$ transients regulate astrocyte-tracheal interactions in CNS. *bioRxiv* https://doi.org/10.1101/865659 (2019).
99. Petravicz, J., Fiacco, T. A. & McCarthy, K. D. Loss of $IP_3$ receptor-dependent $Ca^{2+}$ increases in hippocampal astrocytes does not affect baseline CA1 pyramidal neuron synaptic activity. *J. Neurosci.* **28**, 4967–4973 (2008).
**This study shows that $IP_3R2$ is the main $IP_3R$ subtype in astrocytes, and that $IP_3R2$-null mutant mice lack neurotransmitter-evoked and neuromodulator-evoked $Ca^{2+}$ signals.**
100. Bonder, D. E. & McCarthy, K. D. Astrocytic Gq-GPCR-linked IP3R-dependent $Ca^{2+}$ signaling does not mediate neurovascular coupling in mouse visual cortex in vivo. *J. Neurosci.* **34**, 13139–13150 (2014).
101. Patrushev, I., Gavrilov, N., Turlapov, V. & Semyanov, A. Subcellular location of astrocytic calcium stores favors extrasynaptic neuron–astrocyte communication. *Cell Calcium* **54**, 343–349 (2013).
102. Grosche, J. et al. Microdomains for neuron–glia interaction: parallel fiber signaling to Bergmann glial cells. *Nat. Neurosci.* **2**, 139–143 (1999).
**This study uses serial electron microscopy and $Ca^{2+}$ imaging to identify subcellular compartments called 'microdomains' in Bergmann glial cells (astrocyte-like cells in the cerebellum). These glial microdomains autonomously interact with synapses through $Ca^{2+}$ signalling.**
103. Arizono, M. et al. Structural basis of astrocytic $Ca^{2+}$ signals at tripartite synapses. *Nat. Commun.* **11**, 1906 (2020).
104. Plata, A. et al. Astrocytic atrophy following status epilepticus parallels reduced $Ca^{2+}$ activity and impaired synaptic plasticity in the rat hippocampus. *Front. Mol. Neurosci.* https://doi.org/10.3389/fnmol.2018.00215 (2018).
105. Molotkov, D., Zobova, S., Arcas, J. M. & Khiroug, L. Calcium-induced outgrowth of astrocytic peripheral processes requires actin binding by profilin-1. *Cell Calcium* **53**, 338–348 (2013).
106. Tanaka, M. et al. Astrocytic $Ca^{2+}$ signals are required for the functional integrity of tripartite synapses. *Molecular Brain* **6**, 6 (2013).
107. Clopath, C., Büsing, L., Vasilaki, E. & Gerstner, W. Connectivity reflects coding: a model of voltage-based STDP with homeostasis. *Nat. Neurosci.* **13**, 344 (2010).
108. Hasselmo, M. E. & Stern, C. E. Theta rhythm and the encoding and retrieval of space and time. *NeuroImage* **85**, 656–666 (2014).
109. Eichenbaum, H., Dudchenko, P., Wood, E., Shapiro, M. & Tanila, H. The hippocampus, memory, and place cells: is it spatial memory or a memory space? *Neuron* **23**, 209–226 (1999).
110. Otsu, Y. et al. Calcium dynamics in astrocyte processes during neurovascular coupling. *Nat. Neurosci.* **18**, 210–218 (2015).
111. Lind, B. L. et al. Fast $Ca^{2+}$ responses in astrocyte end-feet and neurovascular coupling in mice. *Glia* **66**, 348–358 (2018).
112. Jain, A., Bansal, R., Kumar, A. & Singh, K. D. A comparative study of visual and auditory reaction times on the basis of gender and physical activity levels of medical first year students. *Int. J. Appl. Basic Med. Res.* **5**, 124–127 (2015).
113. Amano, K. et al. Estimation of the timing of human visual perception from magnetoencephalography. *J. Neurosci.* **26**, 3981–3991 (2006).
114. Matsuhashi, M. & Hallett, M. The timing of the conscious intention to move. *Eur. J. Neurosci.* **28**, 2344–2351 (2008).
115. Nedergaard, M. Direct signaling from astrocytes to neurons in cultures of mammalian brain cells. *Science* **263**, 1768–1771 (1994).
116. Lazrak, A. & Peracchia, C. Gap junction gating sensitivity to physiological internal calcium regardless of pH in Novikoff hepatoma cells. *Biophys. J.* **65**, 2002–2012 (1993).
117. Toyofuku, T. et al. Intercellular calcium signaling via gap junction in connexin-43-transfected cells. *J. Biol. Chem.* **273**, 1519–1528 (1998).
118. Fujii, Y., Maekawa, S. & Morita, M. Astrocyte calcium waves propagate proximally by gap junction and distally by extracellular diffusion of ATP released from volume-regulated anion channels. *Sci. Rep.* **7**, 13115 (2017).
119. Slezak, M. et al. Distinct mechanisms for visual and motor-related astrocyte responses in mouse visual cortex. *Curr. Biol.* **29**, 3120–3127 (2019).
120. Monai, H. et al. Calcium imaging reveals glial involvement in transcranial direct current stimulation-induced plasticity in mouse brain. *Nat. Commun.* **7**, 11100 (2016).
121. Takata, N. et al. Astrocyte calcium signaling transforms cholinergic modulation to cortical plasticity in vivo. *J. Neurosci.* **31**, 18155–18165 (2011).
122. Hirase, H., Iwai, Y., Takata, N., Shinohara, Y. & Mishima, T. Volume transmission signalling via astrocytes. *Philos. Trans. R. Soc. Lond. B Biol. Sci.* **369**, 20130604 (2014).
123. Fuxe, K., Agnati, L. F., Marcoli, M. & Borroto-Escuela, D. O. Volume transmission in central dopamine and noradrenaline neurons and its astroglial targets. *Neurochem. Res.* **40**, 2600–2614 (2015).
124. Oe, Y. et al. Distinct temporal integration of noradrenaline signaling by astrocytic second messengers during vigilance. *Nat. Commun.* **11**, 471 (2020).
125. Jennings, A. et al. Dopamine elevates and lowers astroglial $Ca^{2+}$ through distinct pathways depending on local synaptic circuitry. *Glia* **65**, 447–459 (2017).
126. Corkrum, M. et al. Dopamine-evoked synaptic regulation in the nucleus accumbens requires astrocyte activity. *Neuron* **105**, 1036–1047 (2020).
127. Papouin, T., Dunphy, J. M., Tolman, M., Dineley, K. T. & Haydon, P. G. Septal cholinergic neuromodulation tunes the astrocyte-dependent gating of hippocampal NMDA receptors to wakefulness. *Neuron* **94**, 840–854 (2017).
128. Garaschuk, O., Milos, R.-I. & Konnerth, A. Targeted bulk-loading of fluorescent indicators for two-photon brain imaging in vivo. *Nat. Protoc.* **1**, 380–386 (2006).
129. Nimmerjahn, A., K. F., Kerr, J. N. & Helmchen, F. Sulforhodamine 101 as a specific marker of astroglia in the neocortex in vivo. *Nat. Methods* **1**, 31–37 (2004).
130. Hill, R. A. & Grutzendler, J. In vivo imaging of oligodendrocytes with sulforhodamine 101. *Nat. Methods* **11**, 1081–1082 (2014).
131. Kang, J. et al. Sulforhodamine 101 induces long-term potentiation of intrinsic excitability and synaptic efficacy in hippocampal CA1 pyramidal neurons. *Neuroscience* **169**, 1601–1609 (2010).
132. Fink, S. et al. in *Neuronal Network Analysis: Concepts and Experimental Approaches* (eds Fellin, T. & Halassa M.) 21–43 (Humana, 2012).
133. Henneberger, C., Papouin, T., Oliet, S. H. & Rusakov, D. A. Long-term potentiation depends on release of D-serine from astrocytes. *Nature* **463**, 232–236 (2010).
134. Henneberger, C. & Rusakov, D. A. Monitoring local synaptic activity with astrocytic patch pipettes. *Nat. Protoc.* **7**, 2171–2179 (2012).
135. Gee, J. M. et al. Imaging activity in neurons and glia with a Polr2a-based and Cre-dependent GCaMP5G-IRES-tdTomato reporter mouse. *Neuron* **83**, 1058–1072 (2014).
136. Nakai, J., Ohkura, M. & Imoto, K. A high signal-to-noise $Ca^{2+}$ probe composed of a single green fluorescent protein. *Nat. Biotechnol.* **19**, 137–141 (2001).
137. Akerboom, J. et al. Optimization of a GCaMP calcium indicator for neural activity imaging. *J. Neurosci.* **32**, 13819–13840 (2012).
138. Okubo, Y. et al. Inositol 1,4,5-trisphosphate receptor type 2-independent $Ca^{2+}$ release from the endoplasmic reticulum in astrocytes. *Glia* **67**, 113–124 (2019).
139. Suzuki, J. et al. Imaging intraorganellar $Ca^{2+}$ at subcellular resolution using CEPIA. *Nat. Commun.* **5**, 4153 (2014).
140. Ortinski, P. I. et al. Selective induction of astrocytic gliosis generates deficits in neuronal inhibition. *Nat. Neurosci.* **13**, 584–591 (2010).
141. Atkin, S. D. et al. Transgenic mice expressing a chameleon fluorescent $Ca^{2+}$ indicator in astrocytes and Schwann cells allow study of glial cell $Ca^{2+}$ signals in situ and in vivo. *J. Neurosci. Methods* **181**, 212–226 (2009).
142. Kanemaru, K. et al. In vivo visualization of subtle, transient, and local activity of astrocytes using an ultrasensitive $Ca^{2+}$ indicator. *Cell Rep.* **8**, 311–318 (2014).
143. Hires, S. A., Tian, L. & Looger, L. L. Reporting neural activity with genetically encoded calcium indicators. *Brain Cell Biol.* **36**, 69 (2008).
144. Agronskaia, A. V., Tertoolen, L. & Gerritsen, H. C. Fast fluorescence lifetime imaging of calcium in living cells. *J. Biomed. Opt.* **9**, 1230–1237 (2004).
145. Yellen, G. & Mongeon, R. Quantitative two-photon imaging of fluorescent biosensors. *Curr. Opin. Chem. Biol.* **27**, 24–30 (2015).

### Acknowledgements
The research work of A.S.'s laboratory is supported by Russian Science Foundation grant 20-14-00241. The research work of A.A.'s laboratory is supported by the Chica and Heinz Schaller Research Foundation, the Brain & Behaviour Research Foundation via a National Alliance for Research on Schizophrenia & Depression (NARSAD) Young Investigator Award and grants from the Deutsche Forschungsgemeinschaft (DFG): SFB1134-B01, SFB1158-A09 and FOR2289-P8. C.H.'s laboratory is supported by DFG grants SFB1089 B03, SPP1757 HE6949/1, FOR2795 and HE6949/3.

### Author contributions
The authors contributed equally to all aspects of the article.

### Competing interests
The authors declare no competing interests.

### Peer review information
*Nature Reviews Neuroscience* thanks the anonymous reviewers for their contribution to the peer review of this work.

### Publisher's note
Springer Nature remains neutral with regard to jurisdictional claims in published maps and institutional affiliations.

### RELATED LINKS
**MATLAB:** https://www.mathworks.com/products/matlab.html